



Davide Caramella and Fabio Chiesa

Contents

15.1	Introduction	317
15.2	Signal Characteristics of Tissue Components in MR Images	318
15.2.1	T1-Weighted Images.....	318
15.2.2	T2-Weighted Images.....	318
15.2.3	Water-Fat Signal Decomposition, Fat Suppression, and Dual-Phase Chemical Shift Imaging.....	319
15.2.4	Diffusion-Weighted Imaging.....	320
15.2.5	Contrast-Enhanced Images.....	320
15.3	Fundamentals of Imaging Interpretation: Common Patterns of Disease	321
15.3.1	Fluid-Containing Lesions.....	321
15.3.2	Signal of Blood-Containing Lesions.....	322
15.3.3	Fat-Containing Lesions.....	322
15.3.4	Solid Lesions.....	324
15.4	Essentials of Differential Diagnosis by Anatomical Region	325
15.4.1	Brain Lesions.....	325
15.4.2	Neck Masses.....	329
15.4.3	Evaluation of Mediastinum and Pleura.....	330
15.4.4	Evaluation of Abdomen and Pelvis.....	333
	Further Reading	350

Learning Objectives

- Understand how to distinguish various tissue components based on signal intensity on T1-weighted and T2-weighted images.
- Describe the most common causes of signal alterations on diffusion-weighted images.
- Define an approach to lesion characterization based on identification of four main internal components (fluid, fat, blood, and solid tissues).

- Correlate the most common signal alterations in brain lesions with pathology.
- Correlate the most typical imaging features of cystic and solid lesions in different anatomical regions with pathology.
- Describe the most common signal alterations in the musculoskeletal system.

D. Caramella (✉)

Diagnostic and Interventional Radiology, Department of Translational Research and Advanced Technologies in Medicine and Surgery, University of Pisa, Pisa, Italy
e-mail: davide.caramella@med.unipi.it

F. Chiesa

Unit of Radiology, ASL 5 “Spezzino”, Sarzana, La Spezia, Italy

15.1 Introduction

The definition “hybrid imaging” refers to the combination of cross-sectional imaging techniques used in radiology (CT and MRI) with radionuclide imaging used in nuclear medicine. PET/MRI is a rapidly evolving hybrid imaging technique being increasingly employed in clinical practice and may represent the most challenging modality for nuclear medicine specialists. In the simple PET/CT examination,

low-dose unenhanced CT images are acquired for both attenuation correction and anatomical localization, with a limited contribution for characterizing lesions detected by tracer uptake in the PET scan. In contrast, even the most generic whole body PET/MRI hybrid imaging, without specific organ-targeted or contrast-enhanced sequences, requires interpretation of multiple images including T1-weighted, T2-weighted, and diffusion-weighted images. In the first part of this chapter, the appearance of various tissue components on pulse sequences commonly used in MR examinations will be described, and the most common imaging patterns of disease – classified on the basis of prevalent tissue composition – will be illustrated. In the second part, imaging findings useful for differentiating pathological processes in various organs will be discussed, with particular emphasis on mass lesions commonly evaluated on MRI.

15.2 Signal Characteristics of Tissue Components in MR Images

15.2.1 T1-Weighted Images

Pulse sequence parameters of T1-weighted acquisitions (short TR and TE) create images with contrast between fluids and tissues, both normal and pathological, to create images, based on differences in T1 relaxation characteristics (Table 15.1). Shorter T1 relaxation times correspond to a higher signal intensity on T1-weighted images. Normal tissues that show the shortest T1 relaxation times are composed of molecular species capable of rapid exchange of absorbed radio-frequency energy with the surrounding medium. This is usually achieved through dipolar interactions in a thermodynamically irreversible process generating heat. The most important molecular entities with these properties are:

- Fatty acids, the predominant biochemical constituents of mature adipose tissue
- Water solutions containing dispersed macromolecules, more often represented by proteinaceous and/or mucinous substances that slow random movements of water molecules whose tumbling rate matches the Larmor frequency
- Substances with paramagnetic properties, including gadolinium-based contrast media, specific blood degradation products, and some metallic atoms, such as copper and manganese.

Water solutions with no appreciable proteinaceous or paramagnetic content show very low signal intensity on T1-weighted images.

Parenchymal organs are composed of a mixture of different tissues, which in turn contain a wide range of intra-

Table 15.1 Signal intensities of different body components on T1-weighted and T2-weighted images

Signal intensity	T1-weighted	T2-weighted
High	Fat, highly proteinaceous fluids, gadolinium, methemoglobin, other paramagnetic substances	Clear fluids (e.g., CSF, bile, urine), fat (in TSE sequences)
Intermediate	Most parenchymal organs, muscle tissue, proteinaceous fluids	Most parenchymal organs, muscle tissue
Low	Clear fluids, tendons, ligaments, fibrous tissue	Tendons, ligaments, fibrous tissue
Signal void	Calcium, cortical bone, air	Calcium, cortical bone, air, fast-flowing blood

cellular and extracellular molecules and variable amounts of free water. For this reason all parenchymal organs demonstrate lower T1 signal intensity than fat, with organ-specific differences determined by complex and often incompletely understood biochemical and structural factors.

Muscle tissue has intermediate signal on T1-weighted images comparable to that of some parenchymal organs. Dense fibrous tissue, the main constituent of tendons, ligaments, and mature fibrotic scars, exhibits very low signal intensity on T1-weighted images owing to the low content of free water and strong internal dipolar interactions. Similarly, cortical bone and dense calcium deposits present as signal voids due to the very low density of resonating protons. Gaseous components show no appreciable signal.

Vascular structures usually appear hypointense on T1-weighted images. In specific pulse sequences called “time of flight” a phenomenon known as flow-related enhancement can be exploited to generate angiographic images in which flowing blood shows a markedly high signal intensity.

15.2.2 T2-Weighted Images

Pulse sequence parameters for acquisition of T2-weighted images (long TR and TE) are designed to create image contrast between fluids and tissues, both normal and pathological, based on differences in T2 relaxation time (Table 15.1). Longer T2 relaxation times correspond to a higher signal on T2-weighted images. Molecular tumbling rate and the consequent frequency of dipolar interactions are the main factors influencing the T2 relaxation mechanism.

Free water protons, as found in physiological bodily fluids like bile, urine and cerebrospinal fluid, have the longest T2 relaxation time and thus show the highest signal. In

pulse sequences currently used in clinical practice for obtaining T2-weighted images (such as HASTE, single-shot TSE, and FSE) adipose tissue, mainly composed of fatty acids, shows hyperintense signal, which is slightly lower than water but higher than parenchymal organs. T2-weighted sequences with very long TE can be used to image viscera containing nearly static fluid, with a common example being magnetic resonance cholangiopancreatography (MRCP).

Parenchymal organs demonstrate low to intermediate signal intensity on T2-weighted images. Organ-specific differences are due to variations in tissue composition, especially free water content and concentration of mineral elements such as iron.

Muscle tissue shows lower signal intensity than most parenchymal organs on T2-weighted images. Similar to T1-weighted images, fibrous tissue, cortical bone, and dense calcifications appear dark. Gaseous components exhibit no signal.

Substances with superparamagnetic properties and highly concentrated paramagnetic molecules cause local magnetic field inhomogeneities that accelerate T2 relaxation processes and cause a loss of signal on T2-weighted images. The most notable examples are hemosiderin, the main storage form of iron in tissues, deoxyhemoglobin packed in red blood cells, concentrated gadolinium normally excreted in the urinary tract, and by-products of melanin metabolism in melanocytic tumors.

Vascular structures can show variable signal on T2-weighted images depending on flow characteristics. Rapid flowing blood in arterial vessels usually appears dark because of a flow-related phenomenon denominated “flow void”. However, arterial vessels may show high signal intensity similar to static fluid because of random synchronization of acquired data with the diastolic phase of cardiac cycle. This finding can be typically seen in the aorta and other large arteries running perpendicular to the imaging plane on rapid-shot sequences.

In fluid-attenuated inversion recovery (FLAIR) sequences, signal of static fluids is nulled by precisely timed inversion pulses. FLAIR sequences are used in brain MRI to suppress cerebrospinal fluid signal in order to increase the conspicuity of parenchymal lesions.

Gradient-echo pulse sequences with relatively long TE are weighted for a parameter named T2* (“T2 star”) and are very sensitive to magnetic field inhomogeneities. T2*-weighted sequences are useful to identify small calcifications and superparamagnetic deposits such as hemosiderin, often not detectable on T2-weighted sequences. On gradient-echo T2*-weighted images, calcium and iron deposits appear as very low signal intensity areas with exaggerated size compared to their real volume (“blooming” effect).

15.2.3 Water-Fat Signal Decomposition, Fat Suppression, and Dual-Phase Chemical Shift Imaging

Fat is predominantly composed of medium and long chain fatty acids containing numerous hydrogen atoms linked to a carbon framework which is responsible for the characteristic spectral behavior (difference in precession frequency compared to water) called “chemical shift.” This physical property can be exploited by using particular pulse sequences to achieve specific effects in image contrast.

In Dixon technique, water and fat signal is decomposed to generate three-dimensional images containing signal from a single proton species (“water-only” and “fat-only” images) or a combination of the two. This method is commonly applied to three-dimensional gradient-echo sequences for generating attenuation maps used for correction of PET transmission scan in hybrid imaging.

On fat-saturated sequences and STIR sequences, the signal from fat is suppressed by spectral selective saturation and inversion recovery techniques respectively. On T1-weighted images, fat saturation is commonly applied to three-dimensional fast gradient-echo sequences for breath-hold studies of the chest and abdomen before and after administration of gadolinium-based contrast agents. On T2-weighted fat-saturated sequences, nulling of fat signal increases the contrast resolution of other tissue components and increases the conspicuity of fluid-containing structures. STIR sequences achieve similar results with more complex effects on tissue contrast due to the T1 dependency of inversion recovery technique. The main practical difference between inversion recovery and fat saturation techniques is the low susceptibility of the former to magnetic field inhomogeneities. STIR sequences are therefore advantageous in the study of anatomically complex regions such as the neck and whole body imaging of the skeletal system.

In MR imaging protocols for the evaluation of thoracic and abdominal regions, the most commonly used pulse sequence exploiting the chemical shift effect is dual-phase T1-weighted gradient echo. Two different types of images are obtained at specific TE, depending on magnetic field intensity. In the first, named “out-of-phase” image, water and fat null each other if equally represented in the same image voxel. In the second, named “in-phase” image, water and fat contained in the same voxel combine their signal. Dual-phase chemical shift imaging with in-phase and out-of-phase acquisitions allows recognition of microscopic quantities of fat that occupy less than a voxel, undetectable by selective fat suppression techniques that act on voxels containing predominantly fat. These sequences may also be used to detect substances typically associated with susceptibility artifacts such as iron and calcium deposits; the resulting blooming

effect is more conspicuous on “in-phase” compared to “out-of-phase” images due to the longer TE.

15.2.4 Diffusion-Weighted Imaging

Diffusion-weighted sequences are obtained with the application of symmetrical gradient waveforms before and after a spin-echo refocusing pulse with an echo planar data readout. The extrinsic parameter “*b*-value” determines the sensitivity to molecular diffusion phenomena: a *b*-value of 0 means no diffusion weighting, while progressively increasing *b*-values correspond to higher diffusion sensitivity. In the typical diffusion-weighted imaging protocol, two or three *b*-values are set (from 0 up to a maximum *b*-value of 1000 for most applications), and apparent diffusion coefficient (ADC) maps are generated.

Tissues or pathological processes characterized by a restricted diffusion of water molecules show high signal intensity on high *b*-value diffusion-weighted images. On the other hand, free water (as found in simple fluid-containing structures) appears hyperintense on images with a *b*-value of zero, which are predominantly T2-weighted, and shows no signal on high *b*-value images. In some cases, lesions with high signal intensity on images with a *b*-value of zero may appear bright on moderate to high *b*-value images even if they do not significantly restrict diffusion, a phenomenon known as “T2 shine-through”. ADC maps synthetically and quantitatively convey the information of tissue diffusion characteristics at different *b*-values and prove very useful to avoid the pitfall of T2 shine-through effect.

At low *b*-values ($b < 100$), bulk movement of free water in blood vessels and perfusive components linked to transcapillary diffusion of water dominate over random Brownian movements, determining complete signal loss in vascular structures, called “black blood” effect. Diffusion-weighted images obtained at low *b*-values are mostly used in evaluation of the liver because they allow detection of focal lesions, both benign and malignant, with a high sensitivity. Indeed, small liver lesions may be difficult to identify on T2-weighted images with or without fat suppression due to low contrast between lesion and parenchyma or may be mistaken for a normal vascular structure.

In normal conditions, peripheral lymphoid tissue such as lymph nodes and spleen, shows restricted diffusion and appears hyperintense on high *b*-value images compared to organs like the liver or kidneys. This property makes diffusion-weighted imaging very sensitive for detection of both normal and pathological lymph nodes.

Disease processes that demonstrate restricted diffusion are mostly characterized by:

- High cellularity that correlates microscopically with the presence of many cellular barriers that hinder water diffusion, as found in many malignant and some benign tumors.
- Intracellular edema with relative reduction of extracellular volume as seen in cerebral ischemia.
- Fluid collections with a highly compartmentalized structure like purulent material in abscesses and clotted blood in hematomas.

15.2.5 Contrast-Enhanced Images

Gadolinium-based contrast agents are water-soluble molecules with strong paramagnetic properties that shorten T1 relaxation time of fluid compartments in which they distribute, resulting in signal enhancement. Immediately after intravenous administration, the plasma concentration of gadolinium rapidly rises and reaches a peak in arterial blood vessels followed by a gradual decline as contrast passes in the intravascular compartment and then diffuses in the extracellular space. Multiphase dynamic evaluation of contrast enhancement is commonly performed in MR imaging protocols using fat-saturated three-dimensional T1-weighted gradient-echo sequences that can be acquired in less than 20 s during a single breath-hold. Turbo spin-echo T1-weighted sequences are typically used in static anatomical regions such as the head, neck, spine, pelvis, and limbs.

Images acquired during the maximum arterial concentration of gadolinium are used in contrast-enhanced MR angiography. In late arterial phase, starting about 10 s after arterial peak of contrast, parenchymal organs begin to enhance, with higher contrast enhancement seen in more vascularized tissues such as renal cortex, spleen, and pancreas. In the dynamic contrast-enhanced study of the liver, late arterial phase is called hepatic arterial phase or “portal inflow” phase because portal veins and their branches start to enhance, while hepatic veins remain hypointense. Late arterial phase images are essential in detecting hypervascular lesions in the liver, and for the evaluation of pancreatic pathology.

In images acquired during the venous phase (that starts approximately one minute after gadolinium administration) arterial enhancement decreases, venous vessels progressively enhance, spleen homogeneously enhances, and contrast appears in renal medulla. In the liver, the venous phase is also called portal venous phase because of balanced enhancement between portal system and hepatic veins. In these images the highest contrast between hypovascular lesions and parenchyma can be obtained.

During the equilibrium phase, occurring between three and five min after contrast administration, gadolinium distributes from the intravascular compartment to the interstitial extracellular space. Images in equilibrium phase contribute to the characterization of focal lesions, especially in the liver, based on the pattern and the temporal evolution of contrast enhancement. Lesions demonstrating the “washout” phenomenon, often due to intralesional arteriovenous shunts and altered vascular permeability, appear hypointense compared to parenchyma, while accumulation of gadolinium resulting in hyperintensity may correlate with an increased interstitial space, as commonly found in fibrotic lesions.

Hepatospecific contrast agents are a particular class of gadolinium-based contrast agents that can accumulate in normally functioning liver tissue by a carrier-mediated uptake and be excreted in biliary canaliculi. Contrast-enhanced images acquired in delayed hepatobiliary phase, after a variable time from gadolinium administration (10 min to a few hours depending on the contrast agent), are useful in characterizing liver lesions and in detecting liver metastases. Most gadolinium-based contrast media are predominantly eliminated via glomerular filtration, which can be exploited to visualize the collecting system on images that are acquired in the late urinary excretion phase (more than 5 min after gadolinium administration).

Key Learning Points

- Shorter T1 relaxation times correspond to a higher signal intensity on T1-weighted images.
- Fat and fluids with high proteinaceous and/or mucinous content and paramagnetic substances, including gadolinium-based contrast media, show high signal intensity on T1-weighted images.
- Longer T2 relaxation times correspond to a higher signal intensity on T2-weighted images.

- Simple fluids like bile, urine, and cerebrospinal fluid show high signal intensity on T2-weighted images.
- Substances with superparamagnetic properties like hemosiderin show low signal intensity on gradient-echo T2*-weighted images.
- Dixon technique allows separation of water and fat signal. Fat signal can be nulled on fat-saturated and STIR images.
- Restricted diffusion appears hyperintense on high *b*-value diffusion-weighted images.
- Low *b*-value diffusion-weighted images result in a “black blood” effect that may increase the detection of focal lesions in liver studies.
- Contrast-enhanced images after intravenous administration of gadolinium can be acquired in multiple phases.

15.3 Fundamentals of Imaging Interpretation: Common Patterns of Disease

15.3.1 Fluid-Containing Lesions

Fluid components have variable appearances in different MR pulse sequences. Water solutions with low concentration of macromolecules show the signal typical of clear fluid: marked T2 hyperintensity, T1 hypointensity, and elevated ADC on diffusion-weighted images. Moderate concentrations of macromolecules shorten T1 with minor effects on T2, as typically found in lesions containing proteinaceous or mucinous fluids (Fig. 15.1). Higher concentrations of macromolecules cause T2 shortening that parallels a decrease in signal intensity on T2-weighted images, at times seen only in the dependent portion of a fluid collection due to sedimenta-

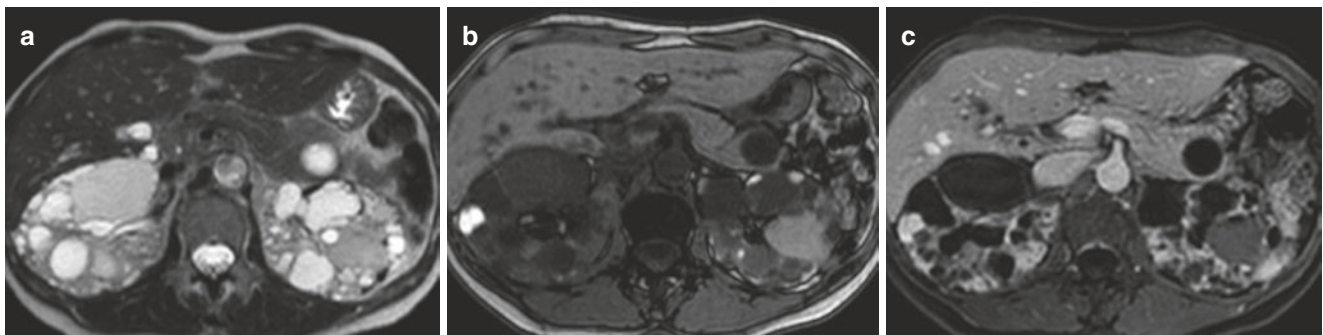


Fig. 15.1 Autosomal dominant polycystic kidney disease. T2-weighted image (a), T1-weighted image (b), and contrast-enhanced image (c) are shown. Multiple cysts of variable size and signal characteristics are seen bilaterally. Increased proteinaceous content or

the presence of blood degradation products determines variable hyperintensity on T1-weighted image and lower signal on T2-weighted image compared with simple cysts

tion phenomena. Restricted diffusion may be seen in corpusculated fluid collections compared to clear fluid.

The presence of blood degradation products may show variable signal characteristics related to their concentration and to the physico-chemical transformation of hemoglobin.

Cysts and cyst-like masses are the most commonly encountered lesions in various anatomical regions, characterized by a predominant fluid content. They may share similar imaging findings despite having different pathological features and clinical significance. Simple cystic lesions appear as clear fluid-containing formations with sharply defined margins, usually round or lobulated contours, thin walls, and no internal structure, with the possible exception of few hairline-thin non-enhancing septa. Benign epithelium-lined true cysts and pseudocysts encapsulated by thin fibrotic walls typically appear as simple cystic lesions. Cyst-like fluid collections of inflammatory origin may be delimited by variably thick walls that enhance after gadolinium depending on vascularity.

Complicated cysts are fluid-containing lesions whose signal characteristics depend on the presence of proteinaceous or bloody material, as seen in hemorrhagic cysts. Abscesses consist of circumscribed fluid collections of infectious etiology containing purulent material that usually appears fluid-like on T1- and T2-weighted images but typically shows restricted diffusion compared with clear fluid. After gadolinium administration a peripheral rim of enhancement is frequently seen surrounding the abscess that may be associated with edema of adjacent tissues, appearing as increased signal on T2-weighted images.

Complex cystic masses are characterized by a predominantly fluid content but show more complex imaging features including thick or irregular walls and internal septations that may enhance after gadolinium, a multilocular appearance with fluid loculations of variable signal intensity, and intralésional solid components originating from the walls and septa.

Some complex masses with a higher proportion of solid enhancing tissue often present as lesions with mixed cystic-solid structure. Solid masses with necrotic or cystic changes show intralésional fluid components and must not be mistaken for complex cystic lesions, usually characterized by more regular-shaped loculations delineated by septa.

15.3.2 Signal of Blood-Containing Lesions

The most common blood-containing lesion is hematoma, whether spontaneous or traumatic. Signal of blood outside the vessel lumen undergoes time-specific changes that reflect the progressive biochemical transformations of blood components. Hematoma signal evolution can be

described by five consecutive phases following hemorrhage: hyperacute (less than 24 h), acute (up to 3 days), early subacute (3 to 7 days), late subacute (up to a month), and chronic.

Hyperacute hematoma shows signal features similar to other fluids, with high signal intensity on T2-weighted images and intermediate to low signal intensity on T1-weighted images due to a higher protein content compared to clear fluid.

Acute-phase hematoma is characterized by deoxygenation of hemoglobin; since paramagnetic deoxyhemoglobin packed inside red blood cells distorts local magnetic fields resulting in signal loss, acute hematomas show decreased signal intensity on T2-weighted images.

In subacute hematoma, the presence of methemoglobin, an oxidation product of hemoglobin with paramagnetic properties that can shorten T1 by interacting with water molecules, causes high signal intensity on T1-weighted images typically starting from the periphery of hematoma and gradually spreading in the central portion as hemoglobin catabolism proceeds and red blood cells lyse.

In the early subacute phase, methemoglobin is concentrated in intact red blood cells causing susceptibility effects similar to deoxyhemoglobin (low signal intensity on T2-weighted images).

In the late subacute phase (Fig. 15.2), red blood cell membranes rupture and release free methemoglobin in the extracellular fluid with disappearance of local magnetic field distortions (hematoma becomes hyperintense again on T2-weighted images). Notably, fat-suppressed T1-weighted sequences are useful to distinguish T1 hyperintense fat that characteristically loses signal from subacute hematoma that remains hyperintense.

In the chronic stage of hematoma evolution there is progressive accumulation of hemosiderin, initially more concentrated at the periphery of the hematoma, with strong superparamagnetic effects that determine low signal intensity on both T1- and T2-weighted images. Gradient-echo T2*-weighted images are very effective for detecting blood products in various phases of degradation owing to their high sensitivity to local magnetic field distortions.

Hemorrhagic phenomena may complicate other focal lesions, both cystic and solid, whose signal characteristics depend on the same processes of blood products degradation as described for hematomas.

15.3.3 Fat-Containing Lesions

For a simplified approach to image analysis of fat-containing lesions, it is useful to consider separately macroscopic and microscopic fat (Fig. 15.3). Macroscopic fat, as found

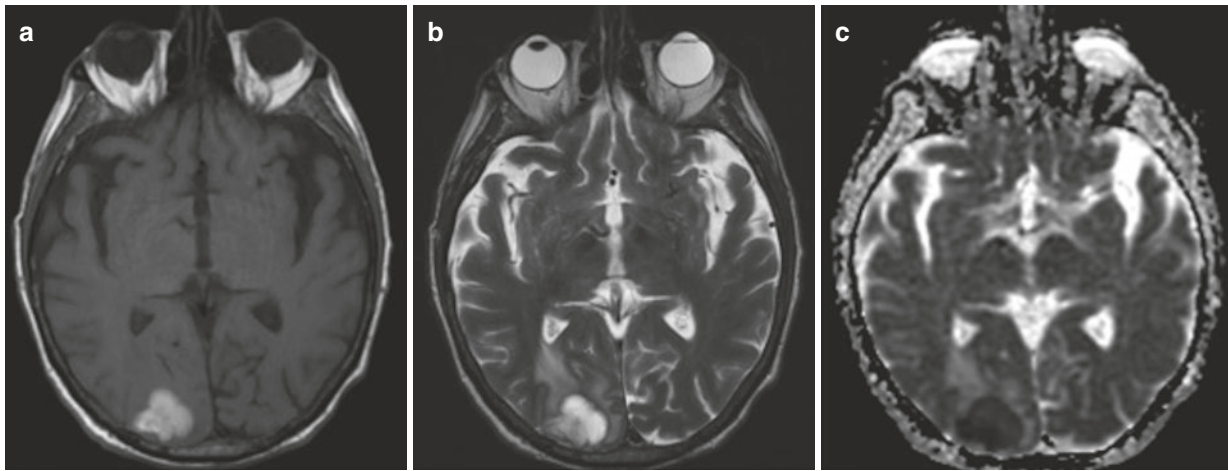


Fig. 15.2 Right occipital lobe subacute hemorrhage. T1-weighted image (a), T2-weighted image (b), and ADC maps (c) are shown. Hyperintensity on both T1-weighted and T2-weighted images is

due to the presence of paramagnetic extracellular methemoglobin. Hemorrhage may exhibit restricted diffusion in its early phases likely due to clot formation

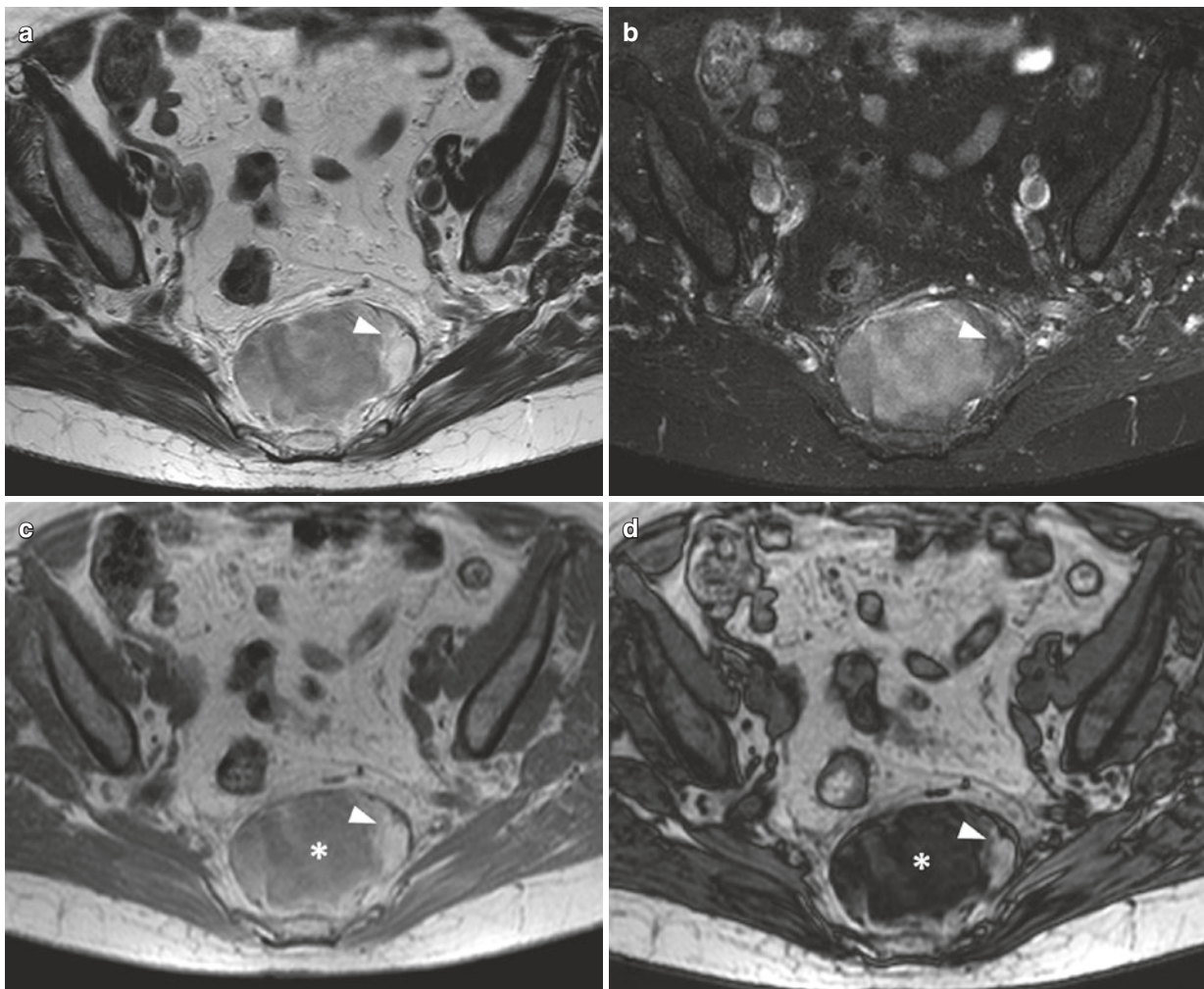


Fig. 15.3 Macroscopic and microscopic fat in a presacral myelipoma. T2-weighted image (a), fat-suppressed T2-weighted image (b), T1-weighted in-phase image (c), and T1-weighted out-of-phase image (d) are shown. An inhomogeneous mass in the presacral region contains large amounts of microscopic fat detectable by the loss of signal on

T1-weighted out-of-phase image (white asterisk). An area of macroscopic fat in the left margin of the mass shows high signal intensity on T1-weighted and T2-weighted images with no signal on the fat-suppressed image (white arrowhead)

in mature adipose tissue and lipomatous lesions, is readily identified by its signal behavior: markedly high signal intensity on T1-weighted images, high signal intensity on T2-weighted TSE sequences, and signal nulling on fat-suppressed images. A mass entirely composed of fat tissue typically shows a thin rim of signal loss on dual-echo chemical shift imaging localized at the interface with surrounding water-containing tissues, denominated “India ink” artifact, caused by similar amounts of lipids and water coexisting in the same voxel. In fact this imaging feature is recognizable at every lipid/water interface such as between parenchymal organs and perivisceral adipose tissue. On T1-weighted sequences employing Dixon technique, fat shows high signal in “fat-only” images and appears dark in “water-only” images, similar to other fat suppression techniques.

Microscopic fat, which may refer to fatty molecules stored in intracellular compartments or very small extracellular fat deposits intermixed with water-rich tissue components in the same voxel, is typically not recognizable on fat-suppressed images but is readily identified by dual-phase chemical shift imaging. Lesions containing microscopic fat show signal loss on dual-phase chemical shift images that is more conspicuous in areas where fat and water are equally represented. A significant predominance of one molecular component over the other may cause a relatively small signal loss, for example, in conditions like mild liver steatosis and inflammatory edema of mesenteric adipose tissue, the latter corresponding to “misty mesentery” appearance on CT.

15.3.4 Solid Lesions

The generic term “solid” refers to a wide spectrum of non-cystic tissue components that may have variable imaging

characteristics correlated with their pathological features. Most entirely or partially solid lesions usually appear mild to moderate hypointense on T1-weighted images and variable hyperintense on T2-weighted images. Contrast enhancement in solid lesions can show variable imaging patterns depending on tissue homogeneity, vascular density and permeability, and extracellular space size.

Certain tissues may have more specific signal characteristics that reflect their distinct pathological features. Tissues characterized by a high cellularity typically show restricted diffusion and may occasionally exhibit low signal intensity on T2-weighted images, as can be found in neoplasms composed of small tightly packed cells with high nuclear-cytoplasmic ratio.

Myxoid tissue, more frequently found in soft tissue tumors, typically appears markedly hyperintense on T2-weighted images, at times approaching the signal of fluid due to the prevalent water-rich extracellular matrix, and in most cases demonstrates a moderate to marked low signal intensity on T1-weighted images. After gadolinium administration myxoid tissue shows mild and progressive enhancement, often with a septal or inhomogeneous lace-like appearance (Fig. 15.4). A minority of solid adenocarcinomas, mostly derived from the gastrointestinal tract, may be predominantly composed of mucinous tissue with imaging features resembling myxoid tissue, characteristically showing unrestricted diffusion.

Dense fibrous tissue that may constitute the main solid component in some tumors typically shows hypointense signal on T2-weighted images and variable signal intensity on T1-weighted images that ranges from nearly isointense to moderately hypointense compared to muscle. Fibrous tissue classically demonstrates a progressive and delayed enhancement due to gradual accumulation of gadolinium in the abundant extracellular space. Immature fibrous tissue, as found in fresh scars, usually shows mildly to moderately elevated signal intensity on T2-weighted images due to interstitial edema

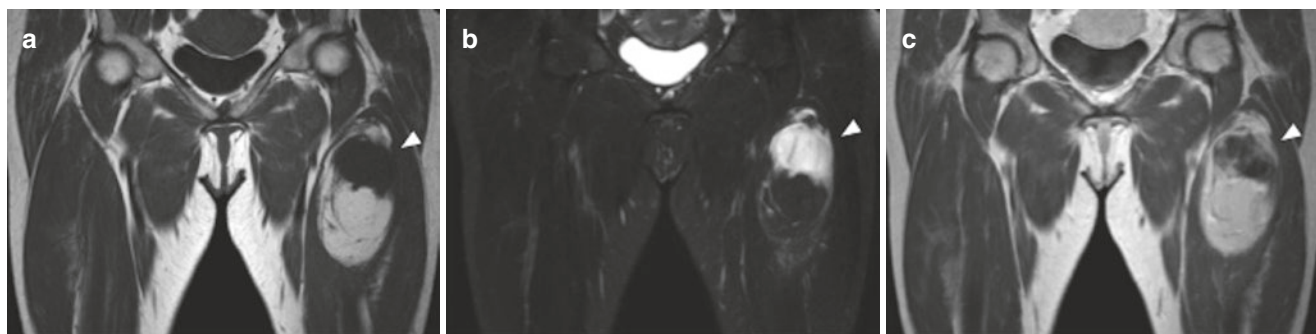


Fig. 15.4 Intramuscular atypical lipomatous tumor of the left thigh. T1-weighted image (a), fat-suppressed T2-weighted image (b), and contrast-enhanced image (c) are shown. The tumor presents as a mass mainly composed of adipose tissue (high signal intensity on T1-weighted

image and low signal intensity on fat-suppressed image). An area most consistent with myxoid tissue shows high signal intensity on T2-weighted image (white arrowhead) and some peripheral and patchy internal enhancement, after contrast administration

and neovascularization often reflected by a more intense contrast enhancement.

Some solid masses contain calcium deposits whose identification may be useful for lesion characterization. While calcifications typically appear as signal voids in all MR images, gradient-echo sequences allow a better detection of small calcium deposits due to the associated blooming effect. In masses with complex structures, solid enhancing tissue can be variably mixed with other constituents like fluid, fat, and blood degradation components. Differential diagnosis of solid lesions relies on recognition of tissue composition together with anatomical location and relevant clinical information.

Key Learning Points

- Simple cysts and cyst-like fluid collections show markedly high signal intensity on T2-weighted images and low signal intensity on T1-weighted images.
- Complicated cysts with proteinaceous or hemorrhagic content show high signal intensity on T1-weighted images and variable signal intensity on T2-weighted images, often lower than simple fluids.
- Purulent material in abscesses shows restricted diffusion.
- Blood components exhibit variable signal features according to their stage of evolution. Deoxyhemoglobin in acute hematomas shows low signal intensity on T2-weighted images. Paramagnetic methemoglobin in subacute hematomas shows high signal intensity on T1-weighted images. Hemosiderin can be detected with a high sensitivity on gradient-echo T2*-weighted images.
- Solid tissues demonstrate variable signal intensity and contrast enhancement features. Myxoid tissue exhibits very high signal intensity on T2-weighted images, whereas fibrous tissue appears markedly hypointense.
- Calcifications appear as signal voids.

15.4 Essentials of Differential Diagnosis by Anatomical Region

15.4.1 Brain Lesions

15.4.1.1 Signal Alterations on T1-Weighted Images

Most brain diseases including vascular, neoplastic, inflammatory, and demyelinating frequently show reduced signal

intensity compared to brain parenchyma on T1-weighted images attributable to a relative increase in free water content. Some pathological processes may show increased signal on T1-weighted images, mostly because of the presence of fat, highly concentrated proteinaceous fluids, mineral deposits, blood components, and other substances with paramagnetic properties whose identification may assist in diagnosis.

Subacute hemorrhagic collections contain paramagnetic methemoglobin that shows high signal intensity on T1-weighted images (Fig. 15.2). Lipomas and dermoid cysts are fat-containing lesions typically located near the midline; the former appear as a non-enhancing mass entirely composed of fat and the latter as a cystic lesion with a T1 hyperintense content due to the presence of fat-rich sebaceous material with variable signal intensity on T2-weighted images and often calcified walls. Dermoid cysts may complicate with rupture and the spread of their fatty content in the subarachnoid space.

Cystic lesions with a highly proteinaceous fluid content that may show high signal intensity on T1-weighted images are more frequently represented by colloid cyst, a round-shaped cyst typically located at the foramen of Monro of third ventricle, and craniopharyngioma often presenting as a complex partially solid-cystic mass in the suprasellar region.

In various toxic-metabolic disorders, mineral substances such as calcium, copper, and manganese can accumulate in certain brain regions, typically in basal ganglia, appearing hyperintense on T1-weighted images. Paramagnetic substances other than gadolinium and methemoglobin that can cause increased signal intensity on T1-weighted images are by-products of melanin metabolism, frequently seen in melanoma metastases. The posterior lobe of hypophysis normally shows high T1 signal intensity and can be easily identified in cases of ectopic position.

15.4.1.2 Signal Alterations on FLAIR and T2-Weighted Images

Most brain pathologies present as hyperintense signal alterations compared to brain parenchyma on T2-weighted and/or FLAIR images mostly due to the increased free water content. Cerebrospinal fluid collections show markedly high signal intensity on T2-weighted images and signal suppression in FLAIR sequences. The most common entities that present as circumscribed clear fluid-filled spaces are dilated perivascular spaces and chronic lacunar infarcts in parenchymal regions supplied by deep penetrating arteries; the latter can be recognized by the presence of a hyperintense rim typically surrounding the fluid cavity on FLAIR images. Arachnoid cysts are relatively common thin-walled cystic lesions of developmental origin located in the subarachnoid space, more commonly in middle fossa, that follow cerebrospinal fluid signal in all imaging sequences.

A wide variety of intra-axial and extra-axial lesions may demonstrate a predominantly cystic appearance with fluid content of variable composition that is often not entirely suppressed on FLAIR images. Epidermoid cysts are pure cystic masses most frequently located in the cerebellopontine angle or suprasellar cisterns that show some FLAIR hyperintensity due to corpusculated content. The most common extra-axial solid tumors, schwannoma and meningioma, may show cystic changes that can occasionally result in a predominantly cystic appearance. Some low-grade primary brain neoplasms can appear as predominantly cystic masses with marked high signal intensity on T2-weighted images, typically associated with a solid component that enhances after gadolinium administration. A variety of neoplastic and infectious diseases can appear as predominantly fluid-containing lesions that may assume a cyst-like appearance.

Metastases, high-grade glial tumors, and abscesses may share similar imaging features including the presence of abundant T2 hyperintense fluid-like components that do not suppress on FLAIR, walls of variable thickness, and mass effect on surrounding structures. These lesions are frequently associated with perilesional vasogenic edema that appears as high signal intensity with a characteristic digitiform appearance (Fig. 15.5). Malignant necrotic neoplasms tend to have thick irregular walls surrounding the central necrotic portion, while abscesses, especially of bacterial etiology, are typically delineated by a thin outer hypointense rim on T2 weighted images. In fact, it is often impossible to distinguish a necrotic neoplasm from a pyogenic abscess on the basis of signal characteristics on T2-weighted and FLAIR images alone. Differential diagnoses include other infectious diseases of variable etiology and require evaluation of diffusion-weighted

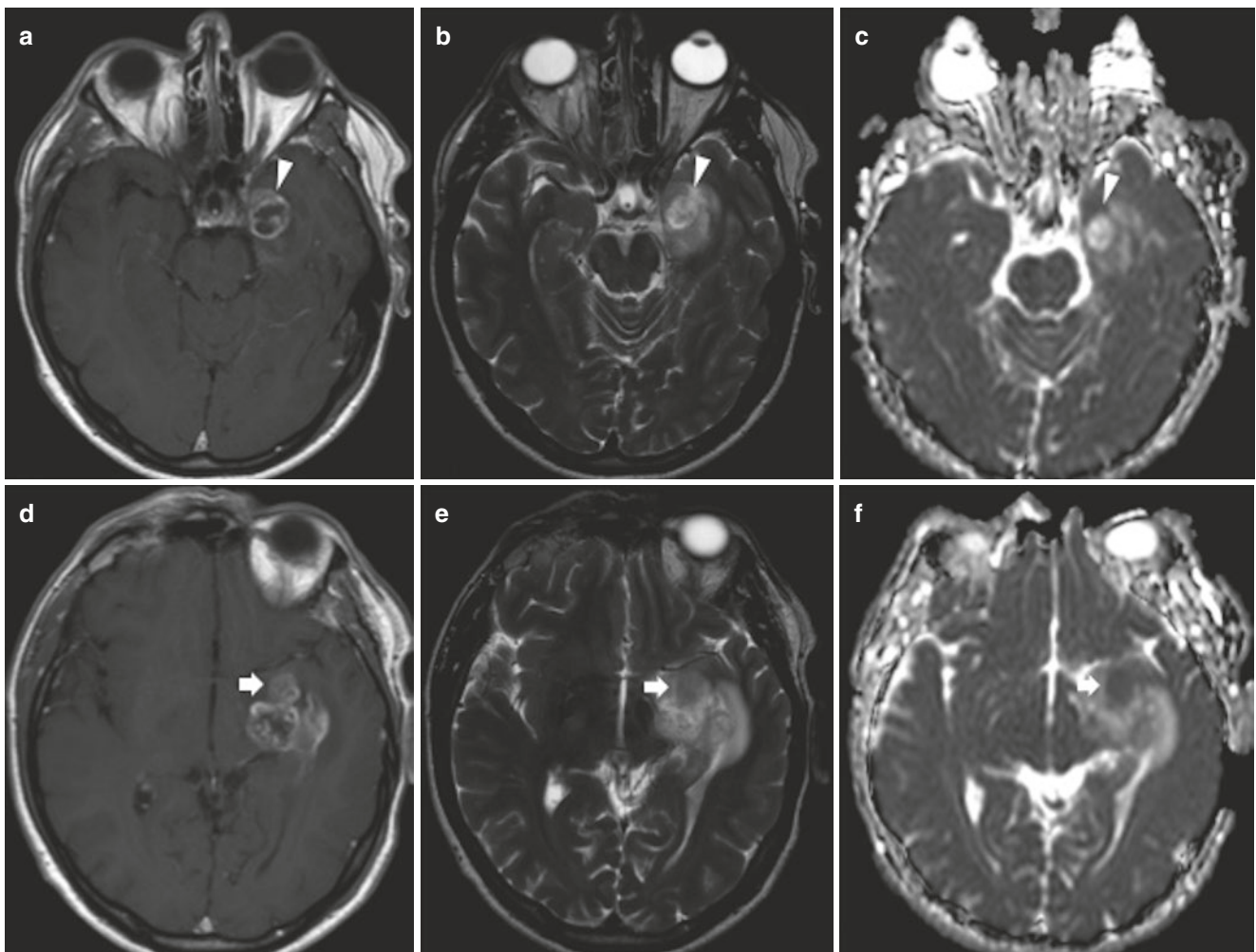


Fig. 15.5 Left temporal lobe glioblastoma. Contrast-enhanced images (a, d), T2-weighted images (b, e), and apparent diffusion coefficient images (c, f) are shown. The tumor appears as an inhomogeneous mass with a rim-enhancing necrotic portion that exhibits unrestricted diffusion (white arrowhead in a, b, and c). In a more cranial slice, a

solid component shows contrast enhancement, relative hypointensity on T2-weighted image, and reduced diffusion compared to adjacent tumor (white arrow in c, d, and e), likely attributable to a higher cellularity

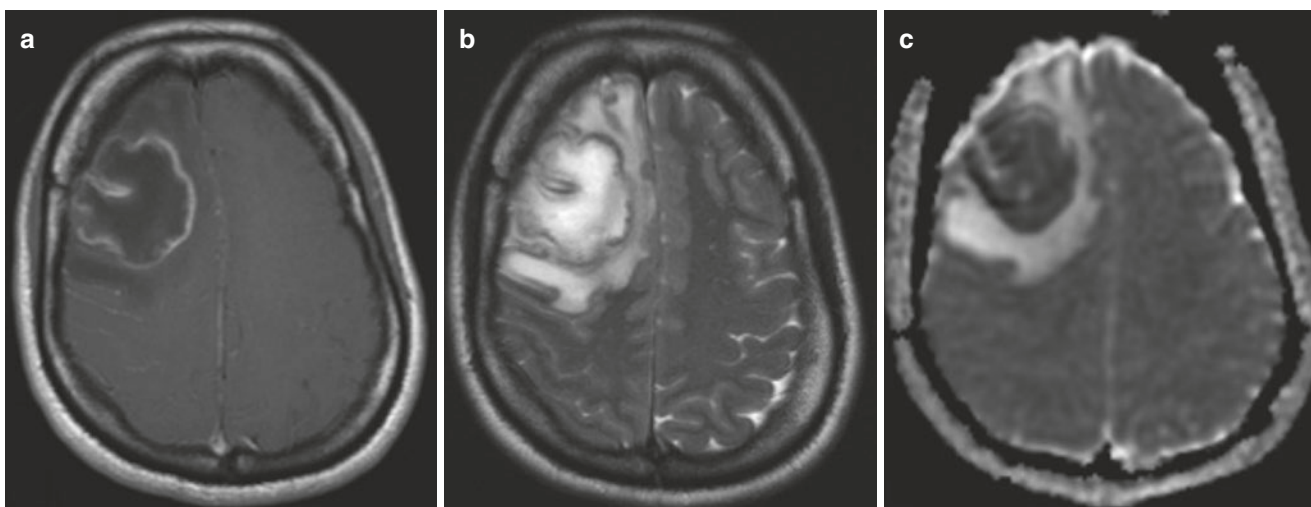


Fig. 15.6 Right frontal lobe abscess. Contrast-enhanced image (a), T2-weighted image (b), and apparent diffusion coefficient image (c) are shown. Abscess presents as a rim-enhancing mass with a central portion

showing hyperintense signal on T2-weighted image and restricted diffusion due to the purulent content. Associated perilesional edema shows high signal on T2-weighted image

images to identify purulent material (Fig. 15.6). Neurocysticercosis often appears as multiple cystic lesion disseminated in brain parenchyma and subarachnoid spaces with variable imaging features according to the disease stage. This has to be distinguished from other multifocal cyst-like masses of infectious and neoplastic origin.

Many other parenchymal diseases show prevalent high signal intensity on T2-weighted and FLAIR images without macroscopic accumulation of fluid. A large number of primary tumors with different clinicopathological features and variable location (intraparenchymal, intraventricular, and extra-axial) often appear as infiltrative masses composed of predominantly hyperintense tissue on T2-weighted images.

Parenchymal territories involved in ischemic infarction show increased signal intensity on T2-weighted and FLAIR images starting in the acute phase and gradually increasing as the necrotic process evolves. Intracranial hemorrhages from various causes, both intraparenchymal and extra-axial, appears predominantly hyperintense on T2-weighted images in the subacute stage (Fig. 15.2).

Disorders primarily affecting white matter, most notably small vessel disease, inflammatory and demyelinating disorders, and leukoencephalopathies, present as areas of high signal intensity on T2-weighted and FLAIR images with variable morphology and spatial distribution and potentially overlapping features. The interpretation of imaging findings in the clinical context is required to reach the correct diagnosis.

A rather limited number of diseases can show a prevalent low signal intensity on T2-weighted images, including:

- Acute hematomas and masses complicated by hemorrhage.

- Areas of high cellularity in some malignant tumors (Fig. 15.5) that may associate with a moderately restricted diffusion, most typically seen in densely cellular tumors such as medulloblastoma and lymphoma.
- Some melanoma metastases due to the T2-shortening effects of intratumoral paramagnetic compounds.
- Cystic lesions with a highly proteinaceous or mucinous content such as colloid cysts.

The high sensitivity of T2*-weighted gradient-echo sequences for susceptibility artifacts generated by calcium and hemosiderin deposits in brain allows detection of small calcifications and foci of hemorrhage that may help in the differential diagnosis of various brain pathologies including tumors, vascular malformations, and vascular pathologies.

15.4.1.3 Signal Alterations in Diffusion-Weighted Images

Diffusion-weighted imaging is an indispensable technique to reach the correct diagnosis in specific brain diseases. The presence of restricted diffusion in acute ischemic stroke is produced by intracellular cytotoxic edema and allows early recognition and estimation of the infarcted area; diffusion then slowly normalizes after the first week. Bacterial pyogenic abscesses can be distinguished from other fluid-containing masses, such as necrotic tumors, because purulent material shows significantly restricted diffusion (Fig. 15.6), while colliquative necrosis resembles clear fluid. Other infectious diseases such as viral encephalitis mainly caused by herpes simplex virus can present with restricted diffusion that typically involves the cerebral cortex of the temporal lobe and insular region. Epidermoid

cysts can be distinguished from more common arachnoid cysts because they show restricted diffusion due their content. Some brain tumors may show restricted diffusion because of a high cellularity, notably lymphomas, that are usually located supratentorially in the periventricular region, and medulloblastomas, that typically occur in posterior fossa near the fourth ventricle. Acute and subacute hematomas may show a variable appearance on diffusion-weighted images; nevertheless a reduction of ADC values is a common finding in early stages of hematoma evolution (Fig. 15.2) and it has to be considered in the differential diagnosis of diffusion-restricting lesions.

15.4.1.4 Common Patterns of Contrast Enhancement

An intact blood-brain barrier impedes significant diffusion of gadolinium in brain parenchyma with the exception of some anatomical regions where this specialized structure is normally absent, notably hypophysis, pineal gland, choroid plexuses, hypothalamic infundibulum, and area postrema. Meningeal layers are extra-axial structures that do not significantly enhance in normal conditions.

Various diseases are characterized by the presence of contrast enhancement that mainly results from a limited number of mechanisms including passage of gadolinium in brain parenchyma due to blood-brain barrier disruption, neovascularization as seen in tumors, and increased capillary permeability in meningeal pathologies. Different disorders tend to be associated with particular patterns of contrast enhancement that must be recognized to reach the correct diagnosis.

Gyriform enhancement appears as a “serpentine” hyperintensity that involves gray matter in cerebral cortex. This pattern is caused by a damaged blood-brain barrier and is typically found in vascular diseases, such as ischemic cerebral infarction in the subacute phase and posterior reversible encephalopathy syndrome, and in infectious processes like viral encephalitis and meningitis, the latter in association with the classical leptomeningeal enhancement.

Ring enhancement, represented by a rim of contrast enhancement surrounding a central region, is the typical pattern of cerebral abscesses (Fig. 15.6), some primary tumors such as high-grade gliomas (Fig. 15.5) and lymphomas in the immunocompromised patient, and metastatic neoplasms. Diffusion-weighted imaging allows to reliably differentiate pyogenic infectious from neoplastic causes. Rim-enhancing lesions are often associated with perilesional vasogenic edema and mass effect. Subacute basal ganglia infarctions and subacute intraparenchymal hemorrhagic collections, both traumatic and non-traumatic, can

appear as ring-enhancing lesions due to blood-brain barrier disruption at the border between hematoma and normal parenchyma.

Tumefactive demyelination is a particular imaging presentation of demyelinating diseases such as multiple sclerosis, appearing as a ring-enhancing lesion. Useful imaging findings that can help in reaching the correct diagnosis are the presence of an incomplete enhancing rim, little mass effect on surrounding structures relative to its size, and a limited perilesional vasogenic edema.

A common pattern found in metastatic disease besides rim enhancement is nodular subcortical enhancement, typical of small lesions that appear as homogeneously enhancing nodules. The distribution of nodular enhancement depends on the preferential dissemination pathways of primary tumor; metastases that spread via the hematogenous arterial route tend to localize in supratentorial gray-white matter junction, while metastases spreading through paravertebral venous plexus preferentially involve posterior fossa structures like cerebellum and brain stem.

Primary brain tumors may show variable contrast enhancement depending on pathological features. In most solid tumors of glial origins contrast enhancement tends to correlate with pathological grade, with some notable exceptions such as oligodendroglioma. Typically enhancing tumors are represented by lymphoma, meningioma, schwannoma, intraventricular neoplasms like ependymoma and choroid plexus papilloma, and tumors arising in pituitary and pineal glands.

The presence of strong nodular enhancement in the wall of predominantly cystic masses is the typical pattern of low-grade fluid-secreting tumors including pilocytic astrocytoma and hemangioblastoma, most commonly located in cerebellar hemispheres, and pleomorphic xanthoastrocytoma and ganglioglioma that are commonly supratentorial.

Enhancement of periventricular subependymal layer can be found in primary central nervous system lymphoma and high-grade glial tumors, the former typically showing intense and often homogeneous enhancement.

Extra-axial diseases involving meningeal layers can show specific patterns of enhancement that can prove useful in narrowing the differential diagnosis. Leptomeningeal enhancement, consisting of hyperintensity of pia-arachnoid complex that follows along the surface of the brain, is typically seen in diseases spreading in the subarachnoid space, such as infectious and carcinomatous meningitis. Leptomeningeal enhancement is commonly associated with high signal intensity of subarachnoid space on FLAIR images.

Pachymeningeal or dural enhancement involves the dura, the outermost layer of meninges surrounding the central nervous system that forms the tentorium cerebelli and falx cerebri. Tumors of meningeal origin like meningiomas typically appear as intensely enhancing extra-axial masses associated with circumscribed area of dural enhancement (“dural tail”), in continuity with the tumor. Dural involvement by metastatic carcinoma and primarily or secondarily disseminated lymphoma often produces a diffuse irregular enhancement that may coalesce to form large enhancing masses. Less common tumors of intra-axial origin abutting pial surface, such as pleomorphic xanthoastrocytoma, can be associated with focal dural enhancement.

Dural involvement may also be found in granulomatous disease of both infectious (e.g., tuberculosis) and immune-mediated (e.g., sarcoidosis) etiology, typically appearing as a pachymeningeal enhancement with a predominantly basal location that may be diffused or localized, sometimes forming dural masses with a plaque-like morphology.

Key Learning Points

- T1 hyperintense brain alterations are mainly represented by fat-containing lesions (e.g., lipoma, dermoid), proteinaceous fluid-containing lesions (e.g., colloid cyst, craniopharyngioma), and subacute hematomas.
- Most brain pathologies appear as hyperintense alterations on T2-weighted and FLAIR images. T2 hypointense brain alterations are mainly represented by acute hematomas, highly proteinaceous fluid-containing lesions (e.g., colloid cyst), and densely cellular tumors (e.g., lymphoma, medulloblastoma).
- Hemorrhage can be readily detected on gradient-echo T2*-weighted images.
- Pyogenic abscesses can be distinguished from necrotic neoplasms due to the restricted diffusion of purulent material.
- Densely cellular tumors (e.g., lymphoma, medulloblastoma) may show restricted diffusion.
- The specific pattern of contrast enhancement may help in the differential diagnosis.
- Rim enhancement is mainly seen in necrotic neoplasms, both primary and secondary, and infections such as pyogenic abscesses.

15.4.2 Neck Masses

15.4.2.1 Cystic Lesions

Cystic masses are frequently encountered lesions in neck imaging. Most cysts, both congenital and acquired, share similar imaging features, and etiology can be suggested by the specific anatomical location in deep neck spaces.

Thyroglossal duct cyst is the most common developmental lesion located in anterior neck that can show variable signal intensity on T1-weighted images due to proteinaceous content. The presence of intracystic solid tissue in a thyroglossal duct cyst should suggest the development of malignancy.

Second branchial cleft cysts are the most frequent branchial cleft anomalies and are typically located in the lateral aspect of the neck, often anterior or medial to sternocleidomastoid muscle. Laryngoceles can appear as completely cystic lesions located in the supraglottic larynx.

Lymphangiomas are developmental cystic masses often originating in the posterior triangle, but they can extend in other adjacent neck spaces when of large size.

Cystic masses in salivary glands are mainly represented by ranula or sublingual gland mucocele and, in the parotid gland, by various congenital and acquired cysts, the latter mainly represented by mucocele and cystic carcinomas.

Tumors that usually appear as solid masses may sometimes appear as partially or predominantly cystic lesions because of intralesional necrosis, hemorrhage, or cystic changes; they are more frequently represented by neurogenic tumors (schwannoma and neurofibroma) and cystic lymph node metastases, typically from papillary thyroid cancer.

Necrotic lymphadenopathy with predominant fluid components can also be caused by infectious diseases, notably tuberculosis. Abscesses, more commonly located in submandibular or retropharyngeal spaces, appear as fluid-containing lesions with a peripheral rim of contrast enhancement, similar to those found in other anatomical sites.

15.4.2.2 Solid Masses

The most common solid masses occurring in the neck are represented by lymphadenopathies that may have variable causes, including metastatic, lymphomatous, and infectious. Both normal and pathologically enlarged non-necrotic lymph nodes have widely overlapping signal features: moderate hyperintensity on T2-weighted and mild hypointensity on T1-weighted images often with restricted diffusion. Imaging findings typically used to differentiate a solid malignant lymphadenopathy from a reactive enlarged lymph node are based on morphologic criteria with limited diagnostic accuracy, including loss of normal architecture with obliteration of the fatty hilum, round shape, irregular cortical thickening, and inhomogeneous signal. Necrotic lymph

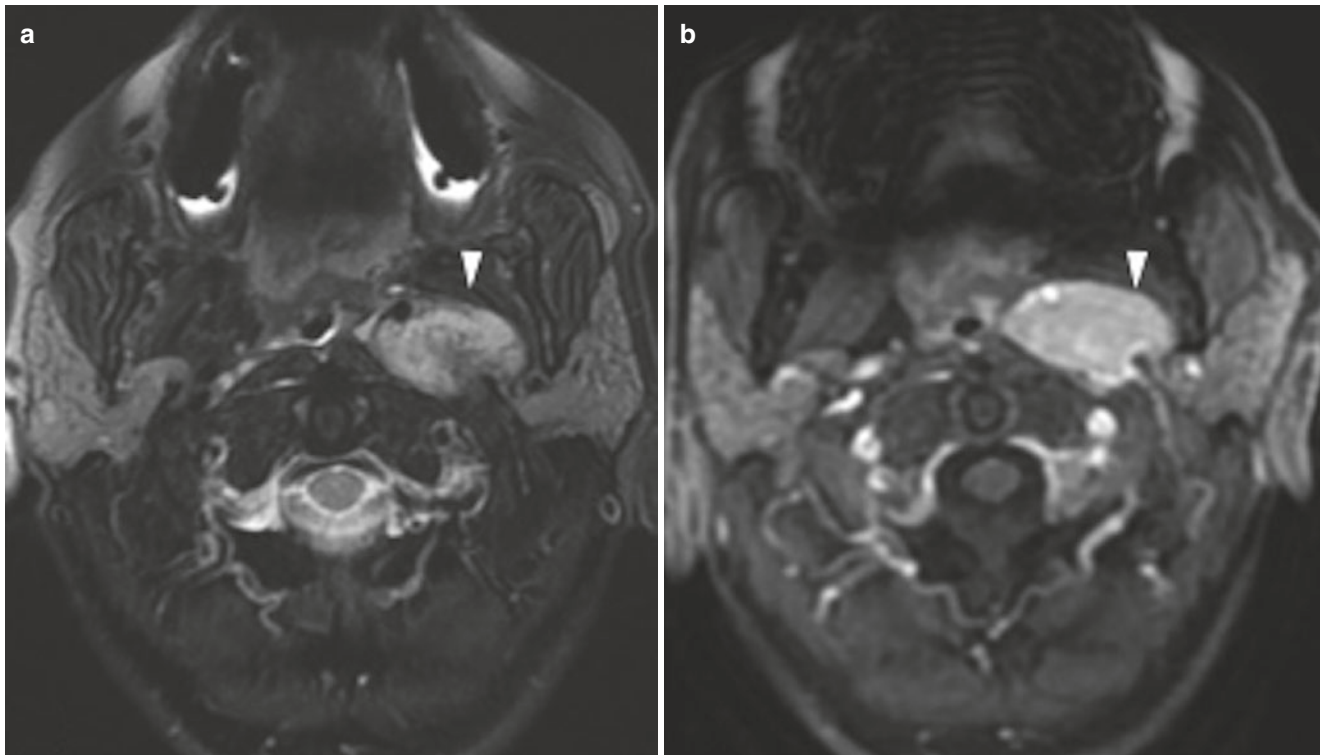


Fig. 15.7 Paraganglioma of the left carotid space. Fat-suppressed T2-weighted images (a) and contrast-enhanced images (b) are shown. The mass (white arrowhead) appears predominantly hyperintense on

T2-weighted image with small low signal foci likely representing flow voids and shows strong contrast enhancement

nodes are characterized by the presence of internal fluid-like non-enhancing components.

Uncommon solid masses that must be distinguished from lymphadenopathies are neurogenic tumors such as peripheral nerve sheath tumors, including schwannoma and neurofibroma, and paraganglioma. Peripheral nerve sheath tumors can have a variable appearance, from homogeneous T2-hyperintense and moderately enhancing lesions to inhomogeneous masses with areas of myxoid degeneration, cystic changes, and hemorrhage, the latter more frequently seen in schwannomas. These tumors, typically located in the carotid space where they may displace the carotid artery and the jugular vein, cannot be reliably distinguished from each other on the basis of imaging characteristics.

Paraganglioma is classically located at the carotid bifurcation (carotid body tumor) and usually causes splaying of internal and external carotid arteries (Fig. 15.7). Paragangliomas can be recognized by their intense vascularity with higher contrast enhancement compared with schwannoma and neurofibroma. A typical imaging feature of paraganglioma on T2-weighted images is the presence of intralesional flow voids giving a “salt-and-pepper” appearance.

MR imaging plays an important role in the evaluation of many other types of mass lesions occurring in the neck for both characterization and staging purposes, including parotid

masses, primary head and neck cancers, and soft tissue tumors.

Key Learning Points

- Cystic lesions of the neck can be readily distinguished from lymphadenopathies and other solid masses on MR images.
- Imaging features correlated with the anatomical location are the mainstay of diagnosis.
- Schwannomas and neurofibromas usually appear as hyperintense on T2-weighted images, moderately enhancing after contrast administration. They may exhibit myxoid degeneration, cystic changes, and hemorrhage.
- A typical imaging feature of paraganglioma on T2-weighted images is the presence of intralesional flow voids giving a “salt-and-pepper” appearance.

15.4.3 Evaluation of Mediastinum and Pleura

15.4.3.1 Mediastinal Masses

Mediastinal cystic lesions can be easily recognized by their smooth margins, fluid content, and thin walls. Pericardial

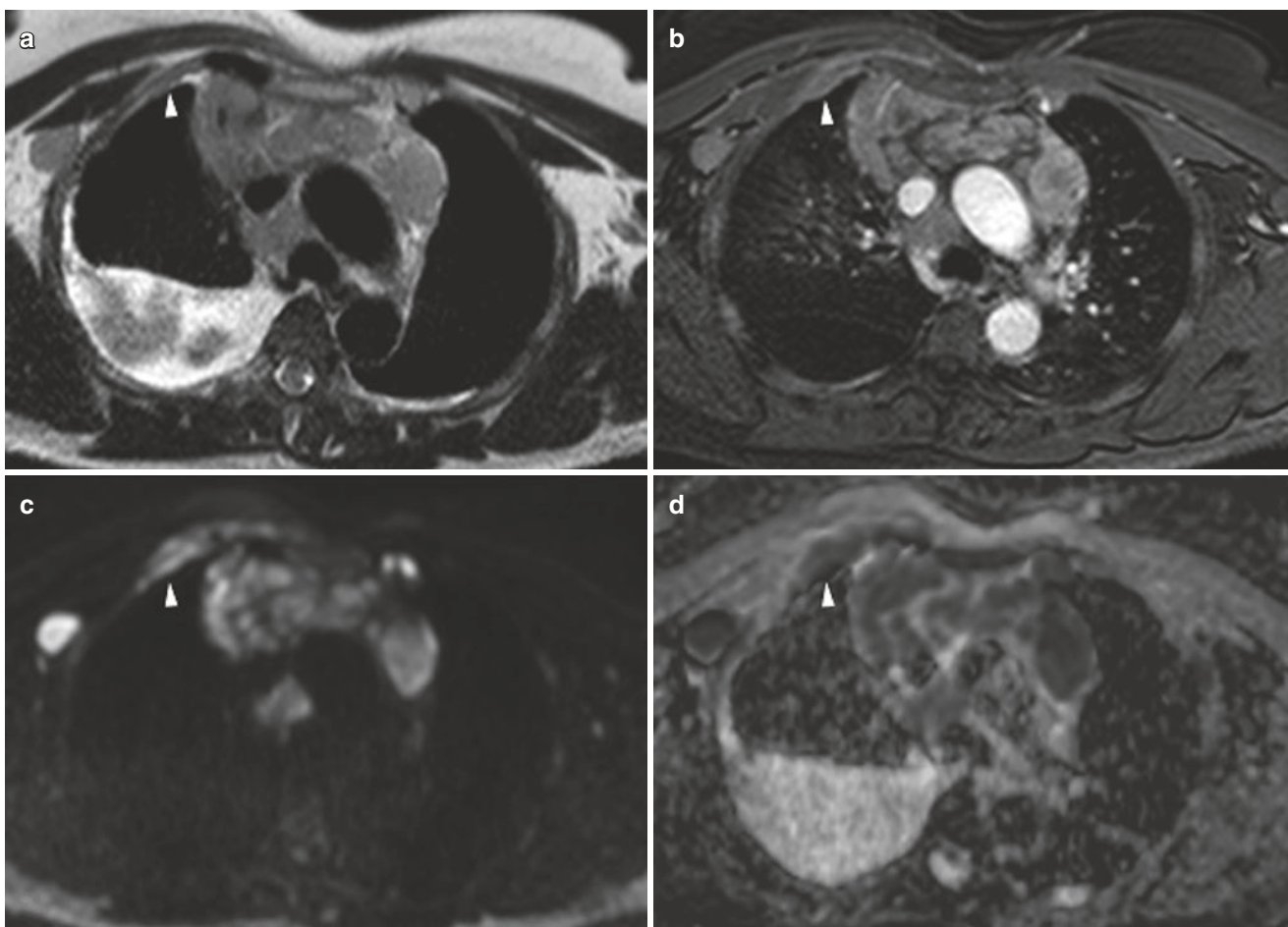


Fig. 15.8 Large B-cell lymphoma with mediastinal involvement. T2-weighted image (a), contrast-enhanced image (b), b-750 diffusion-weighted image (c), and ADC maps (d) are shown. Multiple coalescing lymphadenopathies that encase mediastinal vessels, lymphomatous

infiltration of the anterior chest wall on the right side (white arrowhead), and a right axillary lymphadenopathy can be seen. The lymphoproliferative tissue exhibits intermediate signal on T2-weighted image, slightly inhomogeneous contrast enhancement, and restricted diffusion

cysts present as unilocular cystic lesions in contact with the pericardium, frequently located in right cardio-phrenic angle. Bronchogenic cysts, usually located near the carina, and duplication cysts, often in contiguity with the esophageal wall, present as simple cystic lesions unless complicated by hemorrhage or infection.

The most common fat-containing anterior mediastinal mass is lipoma that shows characteristic imaging features. Teratoma, a benign germ cell tumor, typically located in the anterior mediastinum, presents as complex solid-cystic mass with intralesional fat, sometimes with fat-fluid levels within loculations. Malignant germ cell tumors appear as solid masses with lobulated or irregular margins that can have relatively homogeneous (as in seminomas) or markedly inhomogeneous signal and contrast enhancement (as in non-seminomatous tumors).

Anterior mediastinum is a common site of involvement for lymphoproliferative disorders. Lymphomas typically

appear as solid masses often with smooth or lobulated contours that may encase vascular structures, with appearance that can range from homogeneous signal and enhancement to inhomogeneous masses with areas of necrosis. Lymphomas are frequently associated with mediastinal lymphadenopathy (Fig. 15.8).

Posterior mediastinal masses located in the paravertebral region are most commonly represented by neurogenic tumors, including peripheral nerve sheath tumors (schwannoma and neurofibroma), tumors originating from sympathetic ganglions (ganglioneuroma and neuroblastoma), and paraganglioma. Mediastinal peripheral nerve sheath tumors show the same imaging features as their counterparts occurring in the neck. Ganglioneuromas typically appear as inhomogeneous hyperintense masses on T2-weighted images with hypointense curvilinear bands of fibrous tissue; neuroblastomas appear as heterogeneously enhancing masses often with necrotic areas. Paragangliomas often present as

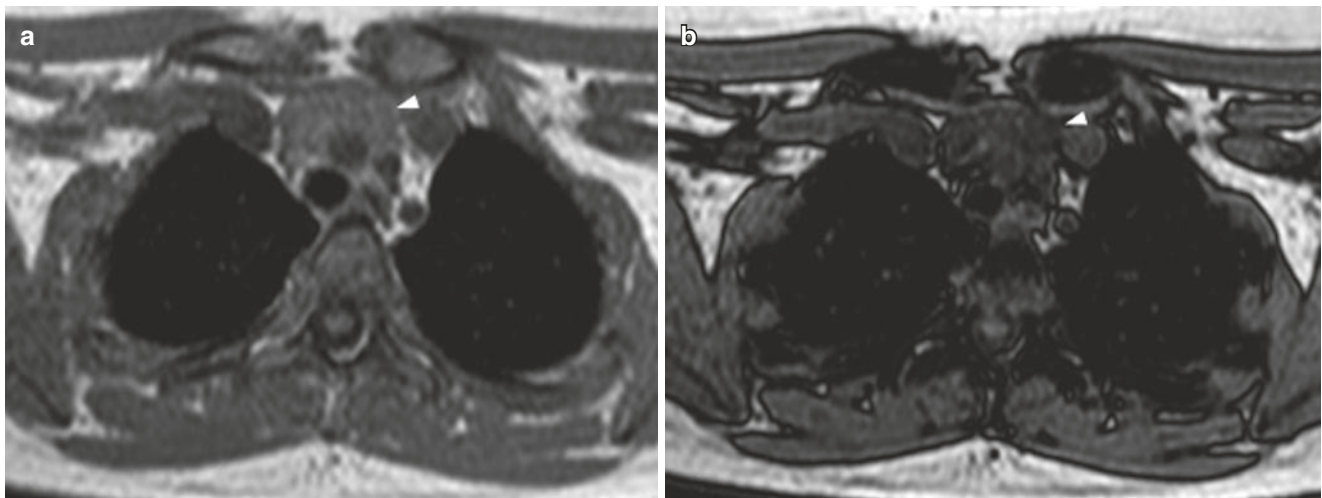


Fig. 15.9 Thymic hyperplasia. T1-weighted in-phase image (a) and out-of-phase image (b) are shown. Hyperplastic thymus loses signal on T1-weighted out-of-phase image (white arrowhead) owing to microscopic fat interspersed between normal thymic tissues

vertically oriented hypervascularized masses with the same signal characteristics as described for carotid body tumors. Mediastinal lymphadenopathies commonly appear as solid enhancing masses with increased signal intensity on diffusion-weighted images (Fig. 15.8). Intranodal fluid-like areas are characteristic of necrotic lymph nodes as can be found in other anatomical sites.

15.4.3.2 Thymic Enlargement

Thymic hyperplasia, both true epithelial hyperplasia and lymphoid “rebound” hyperplasia, commonly presents as a diffuse and symmetric enlargement of thymus. In some cases, enlarged thymus may appear asymmetric or with lobulated contours, thus raising the suspicion of neoplastic disease such as thymic epithelial neoplasia (e.g., thymoma) or lymphoma. Normal and hyperplastic thymus typically contains microscopic fat interspersed within thymic tissue that causes signal loss in dual-phase chemical shift imaging (Fig. 15.9); this feature can be helpful to differentiate hyperplastic enlargement from neoplastic lesions. Congenital thymic cysts commonly appear as simple cystic lesions and sometimes may show T1-hyperintensity because of proteinaceous or hemorrhagic content. Acquired thymic cysts may have multilocular appearance with thin internal septations. The presence of thick septa or solid components within a cystic mass should suggest a cystic thymoma. The presence of abundant fat with minor solid components in a thymic mass is characteristic of benign thymolipoma. Thymic epithelial tumors have variable appearance that can range from round or lobulated homogeneously solid enhancing masses to irregularly shaped infiltrative tumors with inhomogeneous signal and contrast enhancement. Thymic lymphoma may result from secondary involvement or more rarely as an isolated site.

15.4.3.3 Pleural Disease

Magnetic resonance can be a useful adjunct to other diagnostic imaging modalities for evaluation of pleural diseases thanks to its superior contrast resolution. Pleural thickening, especially if it is mild and not circumferential, is an unspecific finding that can be seen in both benign and malignant diseases. Malignant pleural mesothelioma is a relatively rare primary tumor of the pleura associated with asbestos exposure. In patients with asbestos-related pleural disease, thickening of the pleura due to fibrotic plaques or chronic pleuritis often associated with pleural effusion is a frequent occurrence. Distinguishing benign pleural disease from a malignant tumor can be a difficult task in the early stages of mesothelioma. On T2-weighted images, pleural plaques typically show low signal intensity due to abundant collagenous fibrous tissue, often associated with calcifications, while mesothelioma usually appears slightly to moderately hyperintense. Diffusion-weighted images may allow a more accurate diagnosis of pleural mesothelioma in high-risk patients as thickened pleura in mesothelioma usually shows areas of restricted diffusion (Fig. 15.10); this appearance is not specific for malignant mesothelioma and can also be found in metastatic pleural disease.

Key Learning Points

- Mediastinal cystic lesions can be readily distinguished from lymphadenopathies and other solid masses on MR images.
- Imaging features correlated with the anatomical location are the mainstay of diagnosis.
- Thymic hyperplasia can be differentiated from other causes of thymic enlargement due to the pres-

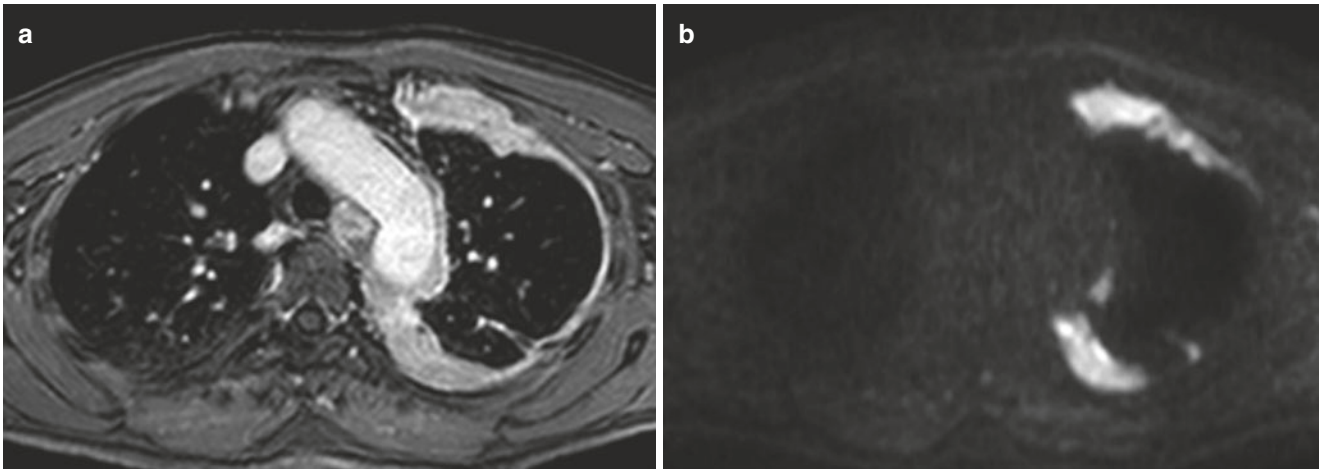


Fig. 15.10 Left malignant pleural mesothelioma. Contrast-enhanced image (a) and b-750 diffusion-weighted image (b) are shown. The irregular pleural thickening shows contrast enhancement and mark-

edly elevated signal intensity on diffusion-weighted image indicating restricted diffusion

ence of microscopic fat detectable on dual-phase chemical shift images.

- Malignant pleural mesothelioma typically appears as pleural thickening with restricted diffusion.

15.4.4 Evaluation of Abdomen and Pelvis

15.4.4.1 Diffuse Parenchymal Alterations of the Liver

Hepatic steatosis, also called fatty liver disease, is a very common pathologic condition consisting of an abnormal increase in the amount of triglyceride molecules stored within intracellular vacuoles in hepatocytes. In most circumstances, steatosis diffusely involves the liver parenchyma, although inhomogeneous fat accumulation with areas of relatively spared parenchyma is a frequent occurrence, sometimes resulting in a patchy appearance. Less common variants of liver steatosis are represented by preferential fat deposition in specific liver territories, typically in the right lobe and rarely in a subcapsular or perivascular distribution. Occasionally, fatty liver disease may mimic a focal liver lesion either because steatosis presents as a circumscribed signal alteration, or because the liver parenchyma is focally spared. Imaging findings in fatty liver disease are consistent with the presence of intracellular fat in affected areas, which is readily detectable on dual-phase chemical shift imaging (Fig. 15.11). Focal fat deposition typically appears as a sharp defined area, with no mass effect on adjacent normal vascular and biliary structures.

Acute inflammatory diseases of different etiology tend to show similarly unspecific imaging findings and their diagnosis requires interpretation in the clinical context. In contrast enhanced images acquired during the hepatic arterial phase, heterogeneous parenchymal enhancement can be seen with areas of transitory enhancement that typically fade to isointensity compared to liver parenchyma in portal venous and equilibrium phase images. On T2-weighted images, hyperperfused areas may show a slightly increased signal intensity that is attributable to parenchymal inflammatory infiltrates. In conditions characterized by diffuse liver inflammation as found in acute hepatitis, a periportal edema with high signal intensity of portal spaces on T2-weighted images is common. In more focal processes like cholangitis, wedge-shaped areas of parenchymal inflammation surrounding dilated intrahepatic biliary ducts are typical findings.

In chronic inflammatory diseases evolving toward liver cirrhosis, imaging findings indicate the presence of parenchymal fibrosis. Cirrhotic liver shows nodular contours, irregular shape with variable involvement of different liver segments, often with relative hypertrophy of the caudate and left lobes, and an inhomogeneous parenchymal pattern due to fibrotic tissue deposition delineating regenerative nodules. Fibrosis is better detected in delayed contrast-enhanced images acquired in equilibrium phase (3–5 min after contrast injection) when the gadolinium-based contrast agent diffuses in the interstitial space and accumulates in fibrous tissue resulting in high signal intensity compared to normal liver parenchyma. In cases of mild fibrosis, liver parenchyma assumes a granular texture attributable to micronodular regenerative hyperplasia; with more severe involvement, a coarser nodular pattern with linear strands of fibrosis and large regenerative nodules can be observed. In some circum-

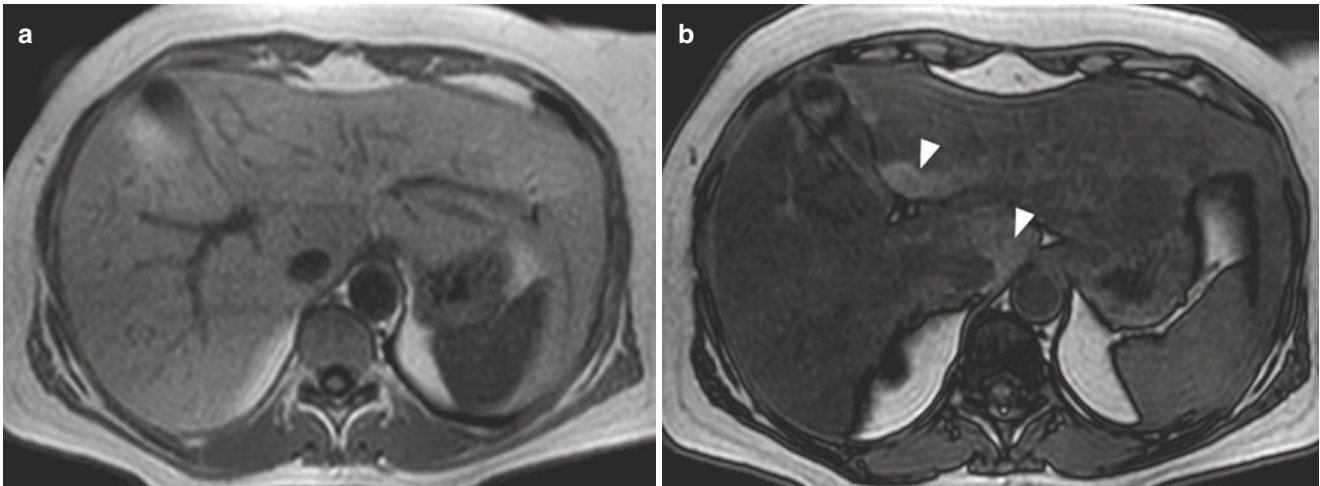


Fig. 15.11 Diffuse hepatic steatosis. T1-weighted in-phase image (a) and out-of-phase image (b) are shown. Liver parenchyma demonstrates marked signal loss on dual-phase imaging due to increased intracellular fat deposition with some areas of fatty sparing (white arrowheads)

stances, fibrotic tissue completely substitutes areas of liver parenchyma and can appear as a focal lesion (so-called confluent fibrosis); useful imaging findings that can suggest a fibrous composition are wedge-shaped margins, preferential subcapsular location, typical delayed contrast enhancement, and mildly to moderately increased signal intensity on T2-weighted images compared to parenchyma probably due to vascular congestion or edema.

15.4.4.2 Focal Liver Lesions

Cystic Lesions

The most common hepatic cystic lesion is represented by simple cyst, a developmental lesion that does not communicate with the biliary system. Simple cysts can be single or multiple and are readily recognized because of their unilocular structure, clear fluid content, round or sometimes lobulated shape with well-delineated margins, and absence of enhancement after contrast administration. Intracystic hemorrhage is a very rare complication in simple liver cysts. Autosomal dominant polycystic liver disease, often associated with cystic kidney disease, appears as multiple cysts that more frequently show a complicated appearance. Developmental lesions with similar appearance are biliary hamartomas, small nodules that do not communicate with the biliary tree and typically present as multiple cysts less than 1 cm in size (von Meyenburg complexes) that may occasionally show a thin rim of contrast enhancement.

A multilocular cystic appearance is typically found in rare neoplasms of biliary origin (cystadenoma and cystadenocarcinoma), pyogenic abscesses, and hydatid disease. Biliary cystadenomas usually show internal septa, thickened

walls, and sometimes mural nodules that enhance after gadolinium administration; the fluid content can have variable signal intensity on T1-weighted images reflecting the presence of proteinaceous, mucinous, or hemorrhagic components. Solid papillary projections and extensive solid components are more frequently observed in malignant cystadenocarcinomas.

Liver abscesses can be unilocular, as more frequently seen in amebic etiology, or have a clustered multilocular appearance generated by the coalescence of multiple fluid-containing areas, more suggestive of pyogenic abscess. Abscesses usually show thick enhancing walls and may be associated with perilesional edema appearing as high signal intensity on T2-weighted images; the purulent fluid content can show restricted diffusion. Hydatid disease in its initial stage can present as a unilocular non-enhancing cystic lesion indistinguishable from simple liver cysts. More typically, hydatid cysts demonstrate a complex internal structure with a thickened pericyst and multiple daughter cysts or intracystic floating membranes (classical “water lily” sign).

Other focal liver lesions can sometimes appear as predominantly or partially cystic. Hepatic benign and malignant masses such as hemangioma and hepatocellular carcinoma can rarely undergo intralesional colliquation or cystic degeneration. Similarly, liver metastases from certain primary tumors may assume a cystic appearance owing to central necrosis or cystic degeneration, such as in melanoma and neuroendocrine tumors, or due to a mucinous histology, more frequently seen in colorectal and ovarian cancer. Nevertheless, liver cystic metastases often show a thin rim of peripheral enhancement or restricted diffusion that is not consistent with the diagnosis of simple hepatic cyst.

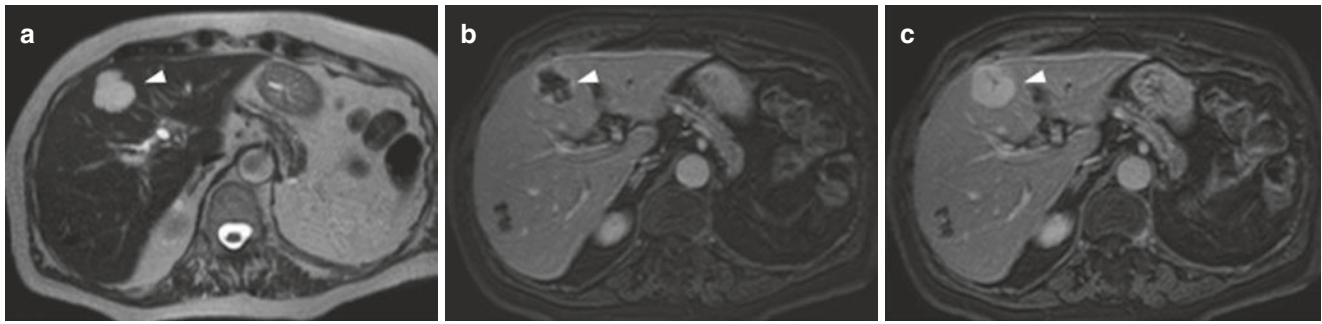


Fig. 15.12 Liver hemangioma. T2-weighted image (a), contrast-enhanced late arterial image (b), and portal-venous image (c) are shown. A well-defined lobulated mass in the right lobe of the liver

(white arrowhead) exhibits markedly high signal intensity on T2-weighted image and early peripheral nodular enhancement with centripetal nearly complete fill-in, consistent with hemangioma

Hepatic Benign Tumors

Besides simple cysts that are the most frequently encountered benign liver focal lesions, some common benign liver tumors can be readily recognized on MRI when they present with typical imaging findings. Hemangiomas are benign masses often incidentally discovered that show very high signal intensity on T2-weighted images, almost reaching the signal of clear fluid due to the presence of dilated vessel filled with slow-flowing blood (Fig. 15.12). On T2-weighted images with long TE, hemangiomas maintain their signal hyperintensity, while more solid lesions such as metastases tend to lose signal compared to fluid-containing structures. After contrast administration hemangiomas typically demonstrate nodular peripheral enhancement with progressive centripetal fill-in that may be incomplete due to central areas of scarring or cystic degeneration. The enhancing portions of hemangiomas reach the same signal intensity as in liver vessels, a useful finding to distinguish hemangioma from malignant lesions that can show a similar centripetal fill-in after contrast administration. Some small hemangiomas do not exhibit the typical nodular centripetal enhancement but rather a complete homogeneous hyperintensity (so-called “flash-filling” hemangioma). This variant of hemangioma may occasionally pose a differential diagnostic problem, since it can appear similar to other focal liver lesions, such as homogeneously enhancing hypervascular liver metastases.

Focal nodular hyperplasia (FNH) is the second most common benign liver lesion. It consists of regenerative hepatic tissue that in most cases manifests as a hypervascular mass with circumscribed margins. A typical imaging feature is the presence of a prominent central scar with fibrous septations and a radiating pattern. FNH usually appears slightly hypointense compared to liver parenchyma with a central scar of low signal intensity on T1-weighted images and nearly isointense with a hyperintense central scar on T2-weighted images. After contrast administration, FNH classically demonstrates a

marked arterial enhancement, with the exception of the central scar, and prevalent isointensity to liver parenchyma on portal venous and equilibrium phases with progressive enhancement of the central fibrous scar. Because of the presence of functioning hepatocytes and the lack of normal biliary canaliculi, FNH tends to accumulate hepatospecific gadolinium-based contrast agents in delayed hepatobiliary phase often resulting in hyperintensity compared to liver parenchyma (Fig. 15.13).

Other focal liver lesions that should be included in the differential diagnosis of suspected FNH are benign and malignant masses with hypervascular appearance, such as flash-filling hemangioma, hepatic adenoma, hepatocellular carcinoma, and hypervascular liver metastases. Among these pathological entities, hepatic adenoma and fibrolamellar variant of hepatocellular carcinoma may show partially overlapping imaging features with FNH. Adenoma may demonstrate a similar appearance on dynamic contrast-enhanced images with hypervascularity in arterial phase, although less intense and homogeneous than FNH and without a central scar, and most frequently appears isointense compared to liver parenchyma in portal venous and equilibrium phase. The most useful imaging feature to differentiate FNH from adenoma is the absence of hepatospecific contrast accumulation on the delayed phase images due to the lack of excretory function resulting in low signal intensity. In addition, adenomas may show variable signal intensity on T1- and T2-weighted images because of excessive intracellular glycogen storage (mild to moderate T1 hyperintensity), intracellular fat deposition (recognizable on dual-phase chemical shift images), and intralesional hemorrhage (signal abnormalities consistent with the presence of blood components).

Hepatic Malignant Tumors

Liver metastases are the most frequently encountered malignant focal solid masses. Metastases often demonstrate a mildly to moderately elevated signal intensity on T2-weighted

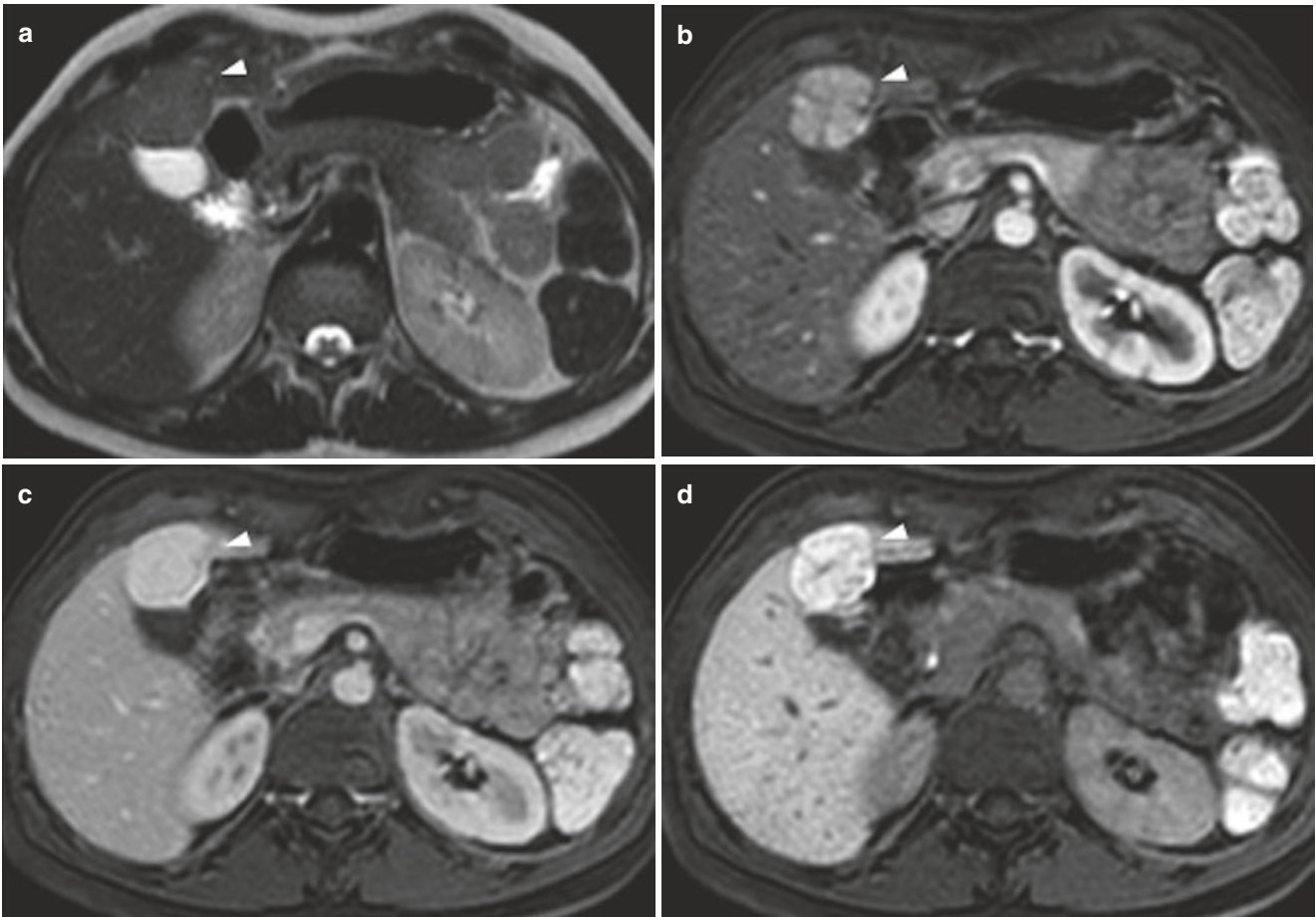


Fig. 15.13 Focal nodular hyperplasia. T2-weighted image (a), contrast-enhanced late arterial image (b), portal-venous image (c), and delayed hepatobiliary image (d) are shown. A solid nodule in the right lobe (white arrowhead) exhibits nearly isointense signal to liver paren-

chyma on T2-weighted image, diffuse arterial enhancement with thin hypointense septa, mild hyperintensity on portal-venous phase, and increased hyperintensity on delayed images

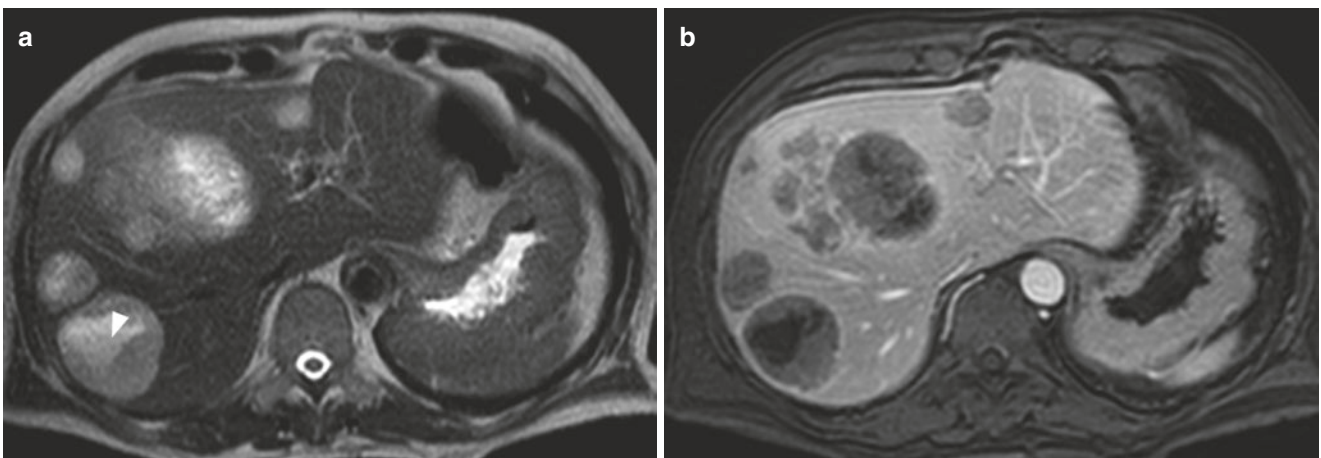


Fig. 15.14 Liver hypovascular metastases from colorectal adenocarcinoma. T2-weighted image (a) and contrast-enhanced portal-venous image (b) are shown. Multiple liver masses exhibit lower

contrast enhancement compared to liver parenchyma with central necrotic changes appearing as high signal intensity areas on T2-weighted image (white arrowhead)

images, which is a useful feature to distinguish metastases from liver cysts and hemangiomas. Larger lesions can show a heterogeneous appearance on T2-weighted images due to necrotic changes or cystic degeneration (Fig. 15.14). On T1-weighted images, metastases are usually hypointense compared to liver parenchyma with some exceptions, such as hemorrhagic metastases or melanoma metastases that show the presence of intracellular paramagnetic substances. Diffusion-weighted imaging has a high sensitivity for the detection of liver metastases and can be useful for lesion characterization despite considerable overlap in diffusion features between solid hepatic lesions, both benign and malignant. In dynamic contrast-enhanced images, liver metastases can have a variable appearance depending on lesion size and pathological features of the primary tumor. Most liver metastases appear as hypovascular focal masses,

enhancing less than the surrounding hepatic parenchyma (Fig. 15.14). Metastases from hypervascular neoplasms, including neuroendocrine tumors, renal cell carcinoma, melanoma, thyroid cancer, and sometimes breast cancer, often demonstrate intense enhancement in the arterial phase images. Small metastases may show a rather homogeneous arterial enhancement and resemble other hypervascular lesions both benign, especially flash-filling hemangioma, and malignant such as hepatocellular carcinoma. A contrast enhancement pattern considered typical for both hypervascular and hypovascular liver metastasis is represented by a peripheral rim of enhancement that can persist or wash out in portal venous or equilibrium phases. The central portion of metastases may show progressive filling with accumulation of contrast that occasionally reach isointensity compared to liver parenchyma although a relative hypointensity is more

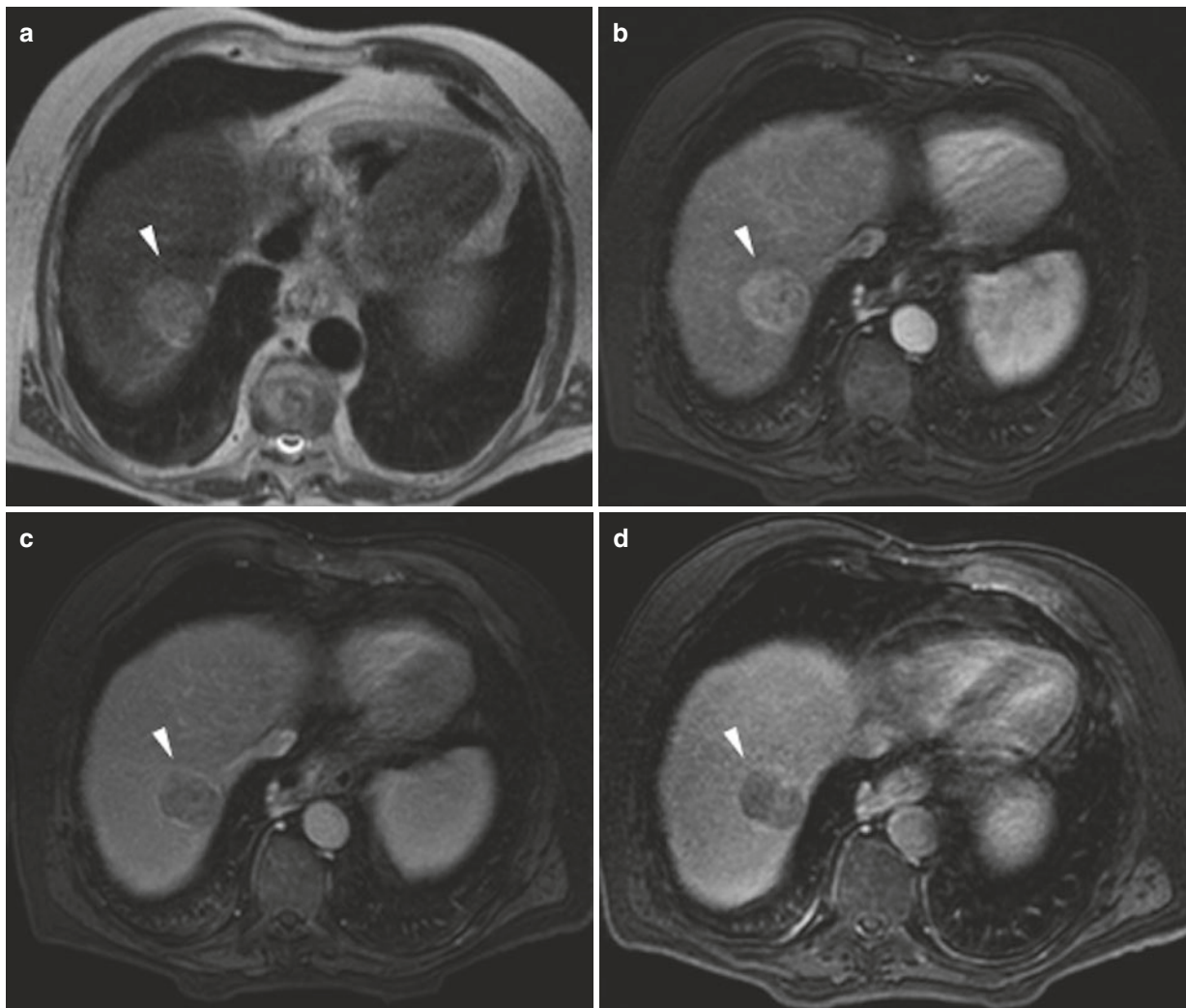


Fig. 15.15 Hepatocellular carcinoma. T2-weighted image (a), contrast-enhanced later arterial image (b), and portal-venous image (c) images are shown. A round mass in the right lobe of the liver (white arrowhead) shows moderately high signal intensity on T2-weighted

image, arterial enhancement with contrast washout and a thin pseudo-capsule in the portal-venous phase, and hypointensity to liver parenchyma in the delayed phase

commonly found. Unlike hemangiomas, metastases demonstrate a continuous peripheral enhancement that may progress centrally with a lower signal intensity compared to blood pool. Larger metastases can show more complex appearances: as an example, large hypervascular metastases can have central areas of necrosis or can show a heterogeneous arterial enhancement that may resemble hepatocellular carcinoma, while hypovascular metastases, typically from colorectal cancer, may present with scalloped margins and internal enhancing fibrous septations that progressively enhance (so-called “cauliflower” appearance).

The most frequent primary malignant tumor of the liver is hepatocellular carcinoma (HCC) that is strongly associated with chronic liver disease and cirrhosis from various causes including viral, exotoxic, autoimmune, and genetic diseases. The typical imaging findings of HCC include a T2-hyperintense mass with arterial enhancement that can be homogeneous in small HCC and markedly heterogeneous in larger tumors, often showing a mosaic-like pattern. On post-contrast images acquired in portal venous and equilibrium phases, HCC usually appears hypointense compared to liver parenchyma as a result of washout, often presenting an enhancing surrounding pseudocapsule constituted by compressed liver parenchyma (Fig. 15.15). In less typical cases, HCC does not show significant washout of contrast and can appear very similar to other benign and malignant hypervascular lesions. In delayed hepatobiliary phase after administration of hepatospecific contrast agents, HCC typically exhibits a lower signal intensity compared to liver parenchyma. Nevertheless, a minority of well-differentiated tumors can uptake and accumulate contrast with consequent hyperintensity on delayed phase images and may be mistaken for FNH. Fibrolamellar carcinoma has traditionally been considered a pathologic variant of hepatocellular carcinoma although it probably represents a distinct clinical entity. Fibrolamellar carcinoma tends to appear as a large heterogeneous hypervascular mass with a central scar that shows low signal intensity on T2-weighted images, in part attributable to calcific deposits. This imaging feature may be helpful to distinguish fibrolamellar carcinoma from FNH, the latter usually showing a T2 hyperintense scar. On post-contrast images acquired on portal venous and equilibrium phases, fibrolamellar carcinoma may appear nearly isointense compared to liver parenchyma or demonstrate washout resulting in hypointensity; the assessment of contrast enhancement on the delayed phase images typically shows lack of contrast uptake with predominant hypointensity, opposite to FNH that characteristically appears iso-hyperintense.

Cholangiocarcinoma is the second more common tumor of the liver. It can present as an intrahepatic mass-forming lesion, a papillary intraductal growth in the biliary tree, or a periductal-infiltrating tumor causing biliary strictures with consequent

extrahepatic cholestasis. Mass-forming cholangiocarcinoma typically presents as a large lesion with mildly to moderately elevated signal intensity on T2-weighted images and low signal intensity on T1-weighted images. After contrast administration, the most frequent finding is an irregular peripheral rim of enhancement with progressive centripetal fill-in that can result in hyperintensity compared to liver parenchyma in equilibrium phase due to abundant fibrous tissue (Fig. 15.16), not to be mistaken for the discontinuous nodular enhancement pattern typically seen in hemangiomas. In the delayed hepatobiliary phase cholangiocarcinomas most commonly exhibit low signal intensity; occasionally, the more fibrotic central portion of the tumor can reach isointensity relative to the liver due to diffusion and retention of gadolinium in the expanded interstitial space.

Key Learning Points

- Fatty liver disease results in signal loss on dual-phase chemical shift images.
- Liver acute inflammatory diseases may manifest with areas of hyperintensity on T2-weighted images and transient parenchymal enhancement in the late arterial phase.
- Liver fibrosis is better appreciated on contrast-enhanced images acquired in the equilibrium phase.
- Simple liver cysts are frequently occurring focal lesions. Multilocular cysts are mainly represented by biliary cystadenoma/cystoadenocarcinomas, pyogenic abscess and hydatid disease.
- Liver abscess usually shows restricted diffusion and peripheral enhancement.
- Liver hemangiomas often show typical imaging features (marked T2 hyperintensity and globular centripetal enhancement).
- Hypervascular benign liver lesions are mainly represented by “flash-filling” hemangiomas, focal nodular hyperplasia (FNH), and hepatic adenomas. FNH often shows typical imaging features with hyperintensity on delayed images obtained with hepatospecific contrast agents.
- Hepatocellular carcinoma presents as a hypervascular solid lesion.
- Liver metastases often show a rim of contrast enhancement on arterial phase images with washout in the portal venous and equilibrium phases.
- Cholangiocarcinoma often shows a peripheral rim of contrast enhancement with progressive centripetal fill-in that must not be mistaken for the nodular enhancement of hemangiomas.

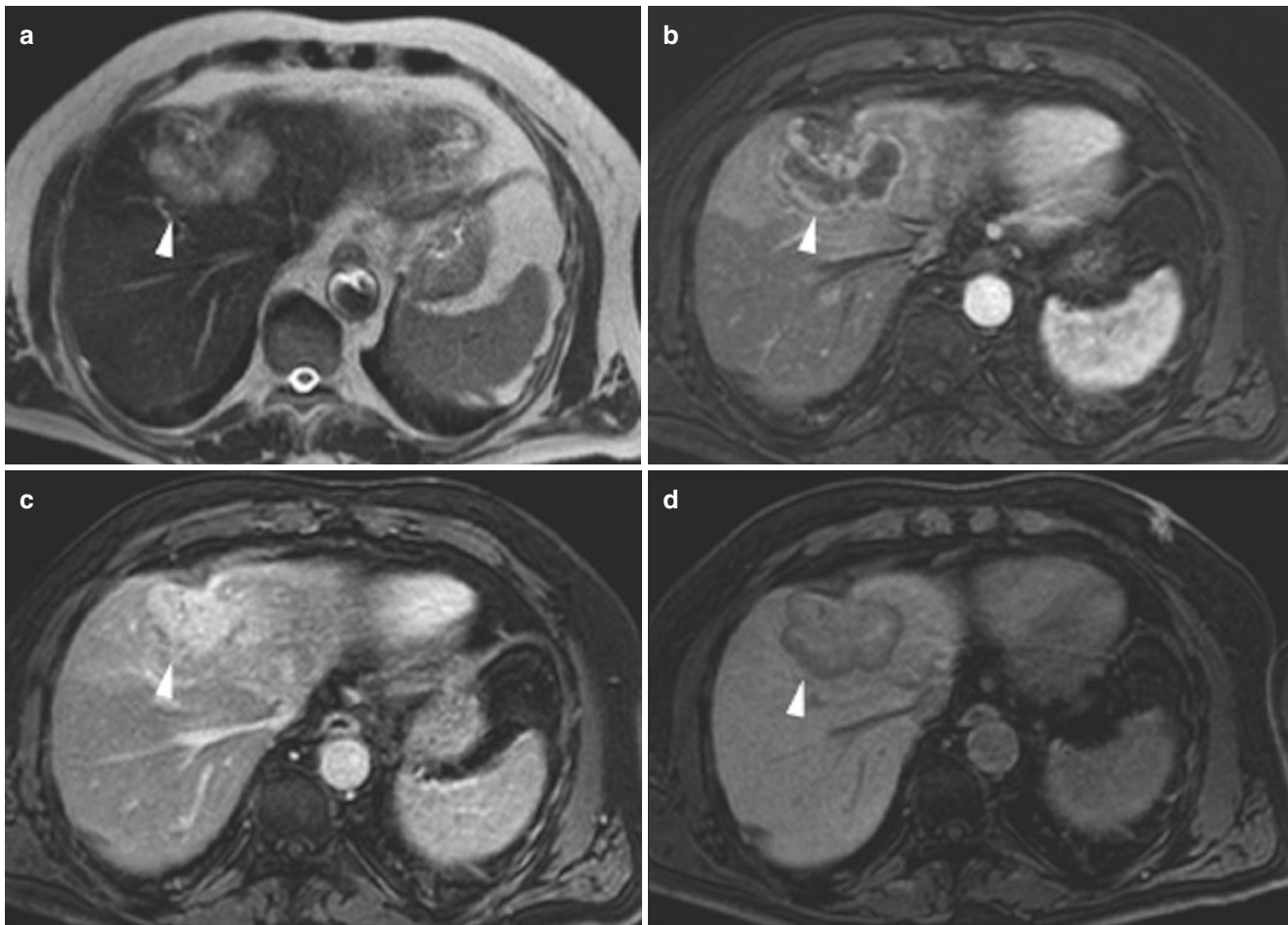


Fig. 15.16 Mass-forming cholangiocarcinoma. T2-weighted (a) and contrast-enhanced images acquired in late arterial phase (b), equilibrium phase (c), and delayed hepatobiliary phase (d) are shown. A mass is seen in the right lobe of the liver (white arrowhead). The lesion exhibits moderate hyperintensity on T2-weighted image, a continuous rim of

contrast enhancement on late arterial phase, and progressive fill-in on equilibrium phase image. In the delayed phase image, the mass appears mainly isointense to liver parenchyma. A thin hypointense rim surrounding the mass and the retraction of liver margin are useful signs to reach the correct diagnosis

15.4.4.3 Pancreatic Masses

Cystic Lesions

The most common cystic lesions of the pancreas are pseudocysts occurring as a complication of pancreatitis. Pseudocysts often appear as unilocular well-circumscribed cystic masses with fluid content and no solid enhancing components with the possible exception of a thin enhancing pseudocapsule. Pseudocysts can be distinguished from walled-off necrosis, a complication of necrotizing pancreatitis, because the latter contains necrotic debris that can deposit in the dependent portion of the fluid cavity, appearing as low signal intensity material on T2-weighted images. The most common cystic pancreatic masses of neoplastic origin are serous cystadenoma, mucinous cystadenoma and cystadenocarcinoma, and intraductal papillary mucinous neoplasm. A multilocular microcystic lesion that can show a “honeycomb” appearance is the typical presentation of

serous cystadenoma, a benign multicystic mass often located in pancreatic head; another classical feature of serous cystadenoma is the presence of a central fibrotic scar that may calcify. Less frequently encountered variants are oligocystic serous cystadenoma that may resemble mucinous cystadenoma and the pseudosolid variant that can mimic a solid neoplasm. Mucinous cystadenomas, typically located in the body and tail of the pancreas, frequently appear as unilocular cysts similar to inflammatory pseudocysts. Sometimes intracystic septa may be present giving a multilocular appearance with fewer large cystic spaces compared to cystadenomas; signal intensity of fluid in loculations can appear similar to simple cysts or show high signal intensity on T1-weighted images due to the mucinous content. Mucinous cystadenoma is considered a borderline lesion with malignant potential; its malignant counterpart, mucinous cystadenocarcinoma, can be distinguished by the presence of solid enhancing tissue.

Intraductal papillary mucinous neoplasms (IPMN) are mucinous neoplasms that grow inside the pancreatic ducts. IPMN can be classified into three types that carry a different prognostic significance: the main duct type, the branch duct type, and the mixed type (combined IPMN). Main duct IPMN, frequently associated with malignant invasive carcinoma, involves diffusely or in a segmental pattern the main pancreatic duct that appears dilated often with lobulated contours. On T2-weighted images, main duct IPMN typically has a fluid-like appearance and may sometimes show intraductal dense mucinous material with low signal, while the presence of solid enhancing nodules should suggest a malignant potential. Branch duct IPMN commonly appears as single or often multiple round or lobulated cysts that directly communicate with the main pancreatic duct, better demonstrated on cholangiopancreatographic T2-weighted images. This is a useful feature in order to differentiate IPMN from other neoplastic cystic lesions. Mixed type IPMN combines imaging features of both main duct and branch duct IPMN. Some solid tumors can uncommonly appear as predominantly or partially lesions, such as ductal adenocarcinoma with cystic degeneration and cystic neuroendocrine neoplasms, the latter characterized in the majority of cases by a thin peripheral rim of viable hypervascular tissue.

Solid Masses

The most frequent solid pancreatic lesion is ductal adenocarcinoma. This tumor often appears as an infiltrating mass that shows low signal compared to pancreatic parenchyma on T1-weighted images and variable signal intensity on T2-weighted images, most often mild hyperintensity. After contrast administration, ductal adenocarcinomas typically exhibits hypovascular features on arterial phase with progressive enhancement in delayed phase related to the abundant fibrous component. The high contrast difference

between tumor and pancreatic parenchyma on T1-weighted precontrast and arterial phase postcontrast images often allows the identification of small lesions that do not alter the pancreatic contour and that may be undetectable with other imaging modalities. For the same purpose, it is also useful the evaluation of secondary signs that could suggest the presence of an infiltrative process, such as abrupt obstruction of the main pancreatic duct with upstream duct dilatation and the “double duct sign,” that refers to dilatation of both biliary tree and main pancreatic duct caused by tumors located in the pancreatic head (Fig. 15.17).

Some benign diseases and pseudolesions may occasionally mimic a malignant mass on imaging, notably focal fatty infiltration and mass-forming chronic pancreatitis; the former can be recognized by the loss of signal on dual-phase chemical shift imaging, while the latter can be indistinguishable from tumor. It is reported that the presence of ductal structures within a mass should suggest focal pancreatitis, while abrupt duct termination at the border of the mass is more consistent with adenocarcinoma; often only biopsy can make a definite diagnosis.

Solid masses other than adenocarcinoma are infrequent and are mainly represented by neuroendocrine tumors and metastases. Neuroendocrine tumors typically appear as single or multiple hypervascular masses that enhance more than pancreatic parenchyma in arterial phase, with variable appearance in portal and delayed phases. Rarely, neuroendocrine tumors show a predominantly cystic appearance usually with a hypervascular enhancing rim. Pancreatic metastases can present as single or multiple masses with signal characteristics and vascularity reflecting primary tumor pathological features; as an example, melanoma and renal cell carcinoma metastases more likely present as hypervascular lesions, while lung or colorectal cancer metastases are typically hypovascular.

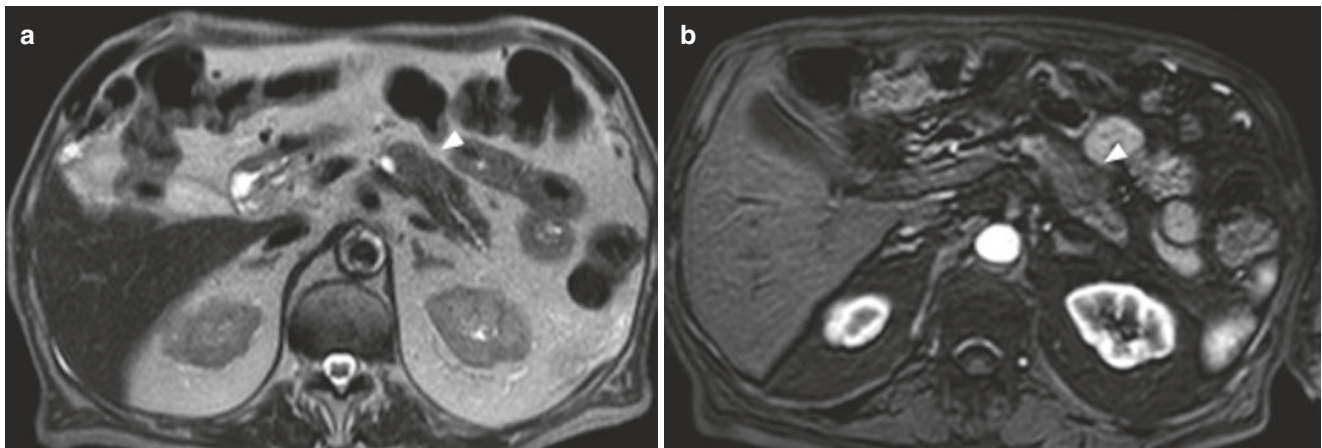


Fig. 15.17 Pancreatic ductal adenocarcinoma. T2-weighted image (a) and contrast-enhanced late arterial phase image (b) are shown. An ill-defined mass in the pancreatic body (white arrowhead) exhibits mild

hyperintensity on T2-weighted image and hypointensity on contrast-enhanced image. The common pancreatic duct distal to the mass appears mildly dilated

Key Learning Points

- Pancreatic cystic lesions are mainly represented by inflammatory pseudocysts, serous and mucinous adenomas, and intraductal papillary mucinous neoplasms. Serous cystadenoma often appears as a multilocular microcystic mass, whereas mucinous adenoma usually presents as a unilocular or multilocular oligocystic mass. Mucinous adenocarcinoma usually shows intralesional solid components.
- The most frequent malignant pancreatic tumor is ductal adenocarcinoma that often appears as a hypovascular mass associated with biliary and/or pancreatic duct dilatation.
- Pancreatic neuroendocrine tumors typically appear as hypervascular masses.
- Pancreatic metastases may be hypervascular or hypovascular depending on the primary tumor.

15.4.4.4 Spleen Masses**Cystic Lesions**

Splenic cysts are the most commonly encountered splenic masses with fluid content; causes may vary from developmental, parasitic, and pseudocyst formation usually from prior hematoma. These lesions typically appear as simple cysts and are often indistinguishable from each other by imaging criteria alone. Parasitic echinococcal cysts can show a multilocular appearance owing to the presence of daughter cysts as often found in other anatomical sites. Splenic abscesses commonly appear as fluid-containing lesions, sometimes with irregular margins and a thin peripheral rim of contrast enhancement; they may be solitary or multiple with unilocular or multilocular appearance. Purulent material in abscesses often shows restricted diffusion and occasionally may be associated with the presence of gas that appears as signal voids and susceptibility artifact better recognizable on dual-phase chemical shift imaging. Splenic hematomas, both subcapsular and intraparenchymal, show the typical signal characteristics of blood collections as found in other organs.

Solid Masses

Hemangioma is the most common benign splenic tumor with imaging features similar to liver hemangiomas; it shows high signal on T2-weighted images and peripheral nodular enhancement in arterial phase with progressive fill-in that

commonly results in homogeneous enhancement in delayed phase. Hamartoma is a rare benign nonneoplastic tumor of the spleen that classically appears as a solitary round-shaped solid mass that demonstrates low signal on T1-weighted images and heterogeneous high signal on T2-weighted images, less intense than typically found in hemangiomas. Hamartoma may show progressive enhancement with accumulation of contrast within dilated sinusoids in delayed phase. In contrast to hemangioma, a diffuse heterogeneous enhancing pattern in arterial phase is usually observed. Because of its rarity, it is often not possible to reliably distinguish hamartoma from other more prevalent solid masses, such as metastases.

The spleen is frequently involved in granulomatous diseases with systemic dissemination, both of infectious and immune-mediated etiology. Splenic granulomas often appear as multiple nodules that are hypointense on T2-weighted images due to a collagenous fibrous component, with mild and typically delayed enhancement after contrast. This appearance should not be confused with siderotic nodules (Gamna-Gandy bodies) that are iron-containing foci usually associated with diseases causing portal hypertension.

Splenic lymphoma is the most common splenic malignancy that can present as a diffuse spleen enlargement or as mass lesions, both solitary and multiple. Imaging features that can rise the suspicion of lymphoma include isointensity or mild hypointensity on T2-weighted images and reduced enhancement compared to spleen parenchyma (Fig. 15.18).

The spleen is an uncommon site of metastatic involvement. Splenic metastases usually present as solitary or multiple nodules, either solid or partially necrotic in their central portion, with variable intensity of enhancement after contrast administration depending on primary tumor. Metastases are commonly hyperintense on T2-weighted images, which can help in differentiating them from lymphoma.

Key Learning Points

- Splenic cystic lesions share similar imaging features.
- Hydatid disease may appear as multilocular splenic cysts.
- Spleen hemangioma is a frequently encountered benign lesion with typical imaging features.
- Granulomatous diseases and lymphomas may appear as splenic nodules with low signal intensity on T2-weighted images.

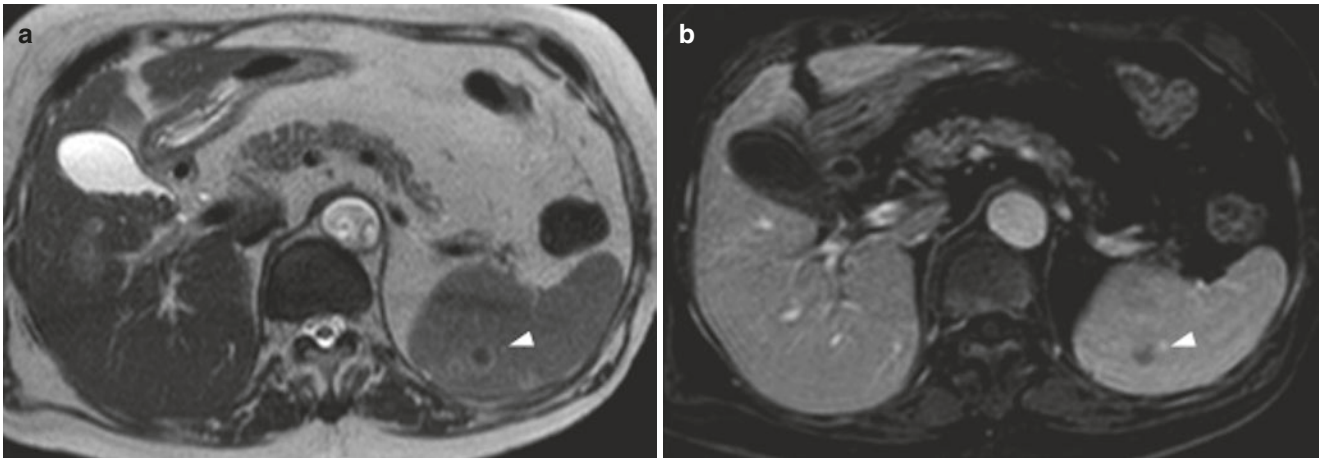


Fig. 15.18 Splenic involvement in Hodgkin's lymphoma. T2-weighted image (a) and contrast-enhanced image (b) are shown. A lymphomatous nodule in the spleen (white arrowhead) exhibits low signal intensity on T2-weighted image and hypointensity after contrast administration

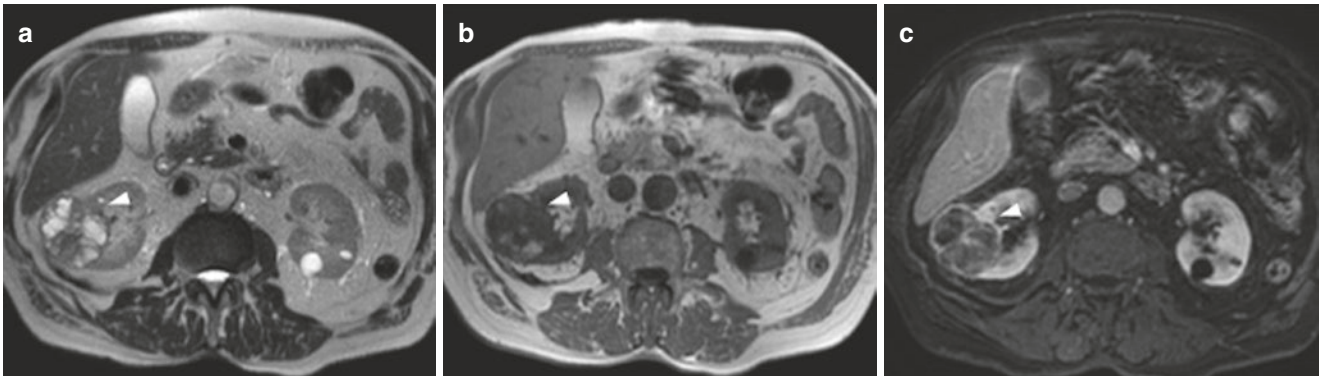


Fig. 15.19 Cystic renal cell carcinoma. T2-weighted image (a), T1-weighted image (b), and contrast-enhanced image (c) are shown. In the right kidney a complex cystic mass (white arrowhead) is seen with

internal septa that demonstrate contrast enhancement and some fluid loculation with high signal on T1-weighted images, likely due to a high proteinaceous or hemorrhagic content

15.4.4.5 Renal Masses

Cystic Lesions

Renal cystic lesions are the most commonly encountered focal lesions of the kidney; they include simple cysts containing clear fluid, complicated cysts with proteinaceous or hemorrhagic content, and complex cysts with thick walls, intracystic septations, and sometimes mural nodules. Simple renal cysts appear similar to other pure cysts found in different anatomical sites; they are often multiple and can be very numerous in polycystic renal disease (Fig. 15.1). A particular type of renal cysts develops in the renal sinus and can have a lymphatic origin (peripelvic cysts) or results from a renal parenchymal cyst extending into the renal sinus (parapelvic cyst). Peripelvic cysts are frequently bilateral and have elongated morphology that can mimic dilated renal calyces and pelvis; contrast-enhanced images acquired in delayed excretory phase allow to differentiate hydronephrosis from peripelvic cysts that can cause stretching and compression of renal calyces. Renal sinus cysts are rarely complicated with hemorrhage or infection.

Complicated cysts show characteristic signal abnormalities; besides hyperintensity on T1-weighted images, they can exhibit low signal on T2-weighted images. Less frequently, chronically complicated cysts can appear pseudosolid due to slightly hyperintense signal on T1-weighted images and near isointense signal compared to renal parenchyma on T2-weighted images; contrast-enhanced imaging can demonstrate the cystic nature of the lesion. Bosniak classification adapted to MR imaging is commonly used to define the risk of malignancy and allow correct management of renal cystic lesions. Simple cyst, cystic lesions with few hairline-thin septa and small complicated cyst without contrast enhancing mural or intracystic component are typically benign. Complex cysts with thick enhancing walls and septations are considered to be at increased risk of malignancy, as they may represent a cystic form of renal cell carcinoma, and are usually surgically excised (Fig. 15.19). About half of complex cysts are constituted by benign lesions such as complicated inflammatory cysts with thick fibrous walls and septa and the rare multilocular cystic renal tumors. Complex cystic masses

with solid enhancing nodules are very frequently malignant and require intervention.

Hematomas and abscesses appear as fluid-containing masses with imaging features similar to those seen in other organs; both lesions may be found inside the kidney, intraparenchymal or subcapsular in location, or involve the perirenal space.

Solid Masses

The presence of contrast enhancement within a renal mass allows to reliably differentiate solid tumors from cystic lesions. Renal cell carcinoma (RCC) of clear cell type is the most common malignant tumor and can have a variable imaging appearance ranging from a predominantly cystic mass (Fig. 15.19), often with a small enhancing mural nodule, to a heterogeneous solid mass with intratumoral necrosis and hemorrhage. Renal cell carcinoma typically shows low signal on T1-weighted images and high signal on T2-weighted images; necrotic changes show fluid-like signal, while hemorrhagic components usually appear hyperintense on T1-weighted images due to the prevalence of blood degradation components in the subacute stage. Some clear cell RCCs have intratumoral deposit of microscopic fat with characteristic signal behavior in dual-phase chemical shift imaging. After contrast administration, most RCCs tend to inhomogeneously enhance during the arterial phase reflecting their hypervascular nature and often show washout of contrast in the following contrastographic phases. The second most common variant of RCC, the papillary type, may be differentiated from its clear cell counterpart because it frequently exhibits low signal intensity on T2-weighted images and demonstrates a lesser degree of contrast enhancement (Fig. 15.20) that sometimes requires assessment of subtraction images between precontrast and post-contrast acquisitions to be recognized. Intratumoral cystic changes and hemorrhage can also be found in papillary RCC. Renal oncocytoma is an uncommon benign solid tumor that cannot be reliably distinguished by clear cell

RCC by imaging alone. The presence of a central stellate scar with high signal on T2-weighted images, a feature often encountered in oncocytomas, represents an unspecific finding that can also be found in RCC. Signs of local venous invasion are helpful to differentiate benign from malignant solid masses.

Renal metastases appear as solid masses with variable enhancement depending on the pathological features of the primary tumor and when solitary may resemble RCC in several aspects. The frequent multifocality and bilateral renal involvement in metastatic disease can suggest the correct diagnosis. Similarly, renal lymphoma usually encountered as part of a disseminated lymphoproliferative disorder often appear as multiple bilateral masses that characteristically show poor contrast enhancement. Less frequently lymphoma presents as a solitary mass that may not be distinguishable from other solid lesions. Other possible patterns of renal involvement include direct invasion from retroperitoneal masses, diffuse renal enlargement, and perirenal soft tissue encasing the kidney.

Renal angiomyolipoma, the second most common benign renal focal lesion after cysts, typically appears as a fat-containing mass. Angiomyolipoma can be reliably diagnosed when macroscopic fat is identified in a renal lesion; while this imaging feature is strongly suggestive of angiomyolipoma, it is not pathognomonic since in rare cases RCCs may contain macroscopic fat, typically associated with foci of calcification or ossification that can help in the differential diagnosis. While most angiomyolipomas are composed predominantly of fat that can be associated with solid enhancing component constituted by vessels and smooth muscle, some appear as lipid-poor angiomyolipomas. These tumors may contain scant amounts of microscopic fat identifiable by dual-phase chemical shift imaging; in some cases, no fat is detectable, and imaging appearance may overlap with other solid renal lesions. Small lipid-poor angiomyolipomas can show low signal intensity on T2-weighted images due to the predominant smooth muscle composition, which can be a

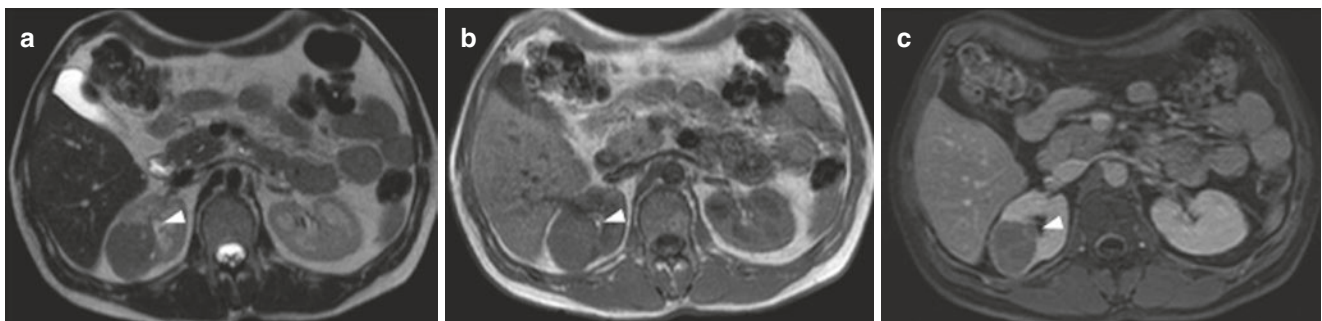


Fig. 15.20 Papillary renal cell carcinoma. T2-weighted image (a), T1-weighted image (b), and contrast-enhanced image (c) are shown. A solid mass located in the right kidney (white arrowhead) appears

hypointense on T2-weighted image, nearly isointense to renal cortex on T1-weighted image, and demonstrates minimal contrast enhancement. These features are suggestive of papillary-type renal cell carcinoma

useful distinguishing feature compared to clear cell RCC that typically appears hyperintense.

Transitional cell carcinomas are malignant tumors derived from the urothelium that may arise in renal calyces and pelvis. These tumors may appear as vegetating lesions located in excretory cavities or as solid masses that infiltrate renal parenchyma and typically determine less alteration of kidney contours compared to renal cell carcinomas.

Key Learning Points

- Simple and complicated renal cysts are frequently occurring lesions with typical imaging features.
- Renal cell carcinomas may appear as complex cystic lesions or as solid masses.
- Papillary-type renal cell carcinomas often show low signal intensity on T2-weighted images, whereas the clear cell type usually appears hyperintense.
- Benign renal oncocytoma cannot be reliably differentiated from renal cell carcinoma on imaging alone.
- Renal angiomyolipomas typically appear as macroscopic fat-containing masses.
- Renal transitional cell carcinomas often exhibit an infiltrative growth pattern with less alteration of kidney contours compared to renal cell carcinomas.

15.4.4.6 Adrenal Masses

Magnetic resonance imaging is particularly useful for characterizing adrenal masses. Adrenal cysts, including true cysts of developmental or parasitic etiology and pseudo-

cysts usually resulting from prior hemorrhage, share the same imaging features of cystic lesions in different anatomical sites.

Adrenal adenomas, both functioning and nonfunctioning, are common benign adrenal lesions that should be distinguished from other benign and malignant solid masses. The typical adrenal adenoma appears as a homogeneous well-margined mass with intermediate signal on T1- and T2-weighted sequences containing abundant intracellular lipids that can be readily detected using dual-phase chemical shift imaging (Fig. 15.21). This imaging feature has been proven to accurately differentiate benign adenomas from metastases. Dynamic contrast-enhanced imaging, with both early and delayed phase images, proved to be useful for identifying lipid-poor adenomas not recognizable with chemical shift imaging; after contrast administration, adenomas tend to show early enhancement followed by contrast washout.

Myelolipoma is a mass lesion composed of a mixture of mature adipose tissue and hematopoietic elements in variable proportions. Some myelolipomas are made almost entirely of adipose tissue, appearing similar to lipomas in different anatomical sites, while others may show a very inhomogeneous composition with predominant solid tissue intermixed with small areas of macroscopic fat. These pathological features correlate with specific imaging findings: adipose tissue signal appears very high on T1-weighted images and is nulled on fat-suppressed images, while hematopoietic tissue shows intermediate signal on T1- and T2-weighted sequences, enhances after contrast administration, and often loses signal on dual-phase chemical shift imaging due to the microscopic fat content.

Pheochromocytomas are neuroendocrine tumors that can show variable signal characteristics; in the most typical

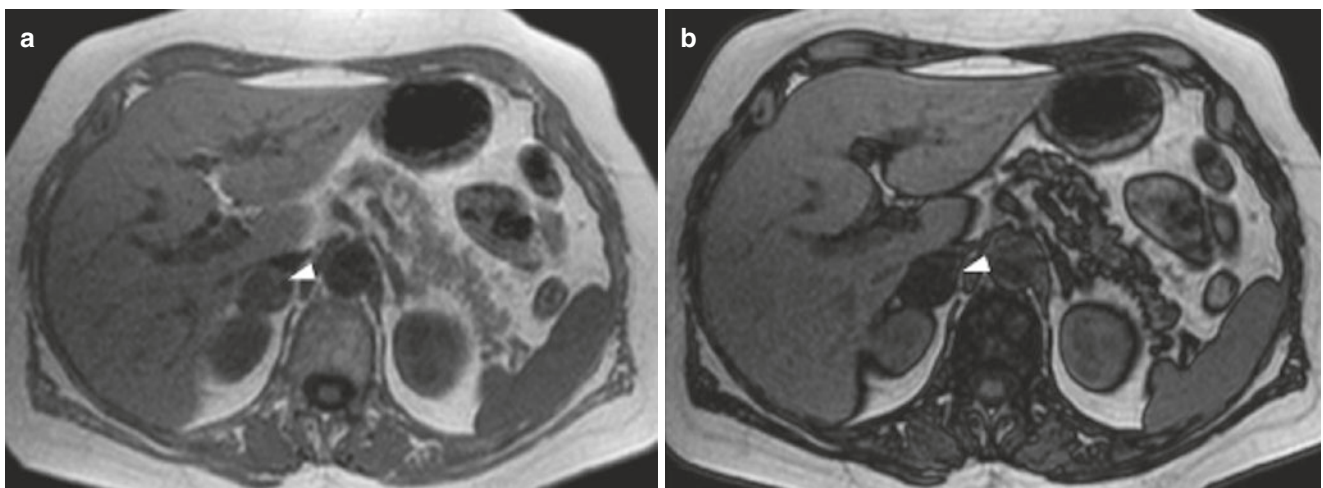


Fig. 15.21 Adrenal adenoma. T1-weighted in-phase image (a) and out-of-phase image (b) are shown. Adenoma in the right adrenal gland (white arrowhead) exhibits a significant signal loss on dual-phase imaging due to the large amount of intracellular fat

cases, they show a markedly high signal intensity on T2-weighted images resulting in the so-called “light bulb” appearance. This feature is neither sensitive nor specific since many pheochromocytomas have intermediate signal on T2-weighted images. Pheochromocytomas often have strong contrast enhancement with prolonged retention of contrast, although a washout enhancement pattern similar to adenoma can sometimes be seen. Large tumors often appear heterogeneous due to the presence of necrotic changes or hemorrhage with variable signal intensity depending on the stage of evolution. In a minority of cases, pheochromocytomas can appear as an entirely cystic lesion with a thin peripheral rim of contrast enhancement that can assist in differential diagnosis with simple cysts.

Adrenal metastases can have variable morphology from well-defined round solid nodules to irregular heterogeneous masses and frequently show bilateral adrenal involvement. Metastases commonly exhibit high signal intensity on T2-weighted images without significant signal loss on dual-phase chemical shift images. In rare cases, metastases from certain types of tumors, such as renal cell carcinoma and hepatocellular carcinoma, may contain microscopic fat showing signal loss in chemical shift imaging, but it is usually less conspicuous compared to adenomas. Larger metastases can show necrotic or hemorrhagic changes.

Adrenal lymphomas appear as solid masses with imaging features that can be indistinguishable from metastases. Adrenocortical carcinomas typically present as a large irregular-shaped mass with predominantly high signal intensity on T2-weighted images and a heterogeneous appearance due to the coexistence of solid enhancing tissue and areas of necrosis and hemorrhage. Adrenocortical carcinomas may contain microscopic fat detectable by dual-phase chemical shift images and less frequently macroscopic fat deposits; nevertheless, their marked inhomogeneous composition allows in most cases distinction from other fat-containing masses such as adenoma and myelolipoma. Neurogenic tumors like neuroblastomas usually appear as solid masses with heterogeneous signal intensity and contrast enhancement due to cystic changes, calcification, and hemorrhage.

Key Learning Points

- Adrenal adenomas can often be differentiated from other solid masses, such as metastases, owing to their microscopic fat content detectable on chemical shift imaging.
- Adrenal myelolipomas are macroscopic fat-containing benign tumors.
- Adrenal pheochromocytomas usually show intense contrast enhancement and high signal intensity on T2-weighted images.

15.4.4.7 Ovarian Masses

Cystic Lesions

Magnetic resonance imaging is a widely used diagnostic tool to evaluate mass lesions in the female pelvis, most commonly represented by cystic lesions of the ovaries. Ovarian follicles and corpora lutea, often incidentally discovered on imaging in premenopausal women, are normal structures developing during the menstrual cycle that have to be distinguished from pathological cystic lesions. Normal follicles appear as simple cysts that can grow in size up to 3 cm and then spontaneously rupture to release the ovocyte and transform into the corpus luteum. Corpus luteum typically appears as a small oval mass less than 3 cm in diameter with thickened walls and crenulated contours that enhance after contrast administration, hyperintense on T2-weighted images but with lower signal intensity compared to clear fluid. The most frequently encountered ovarian cystic lesions larger than 3 cm are functional cysts, either follicular cysts, which resemble a simple cyst or corpus luteum cysts that may exhibit high signal intensity on T1-weighted images due to hemorrhage. Endometrioma, a localized form of endometriosis, typically appears as a cystic lesion with hemorrhagic content that should be distinguished from a complicated functional cyst. Endometriotic cysts usually show high signal intensity on T1-weighted images and low signal intensity on T2-weighted images due to the presence of highly concentrated blood degradation components from recurrent hemorrhage (Fig. 15.22). Sometimes, a fluid-fluid level can form in the endometrioma with low T2 signal intensity in the dependent portion of the cyst due to sedimentation of blood cells and proteinaceous material with a layered appearance.

A particular type of benign ovarian cystic mass is represented by mature cystic teratoma, a fat-containing lesion of germ cell origin. Mature teratoma classically presents as a cyst with a fluid content mainly composed of sebaceous material that has the same signal as fat in all imaging sequences. A solid protuberance projecting from the cyst wall (dermoid plug or Rokitansky nodule) with inhomogeneous signal due to variable tissue composition is a typical finding. In rare cases, the cystic content of mature teratomas may appear similar to clear fluid and mimic a simple cyst of other etiology; in these circumstances, a fat component within the cyst wall or within a Rokitansky nodule is usually seen and can assist in the diagnosis. The presence of prominent solid enhancing components within a partially cystic fat-containing mass is considered suspicious for immature or malignant teratoma.

Ovarian tumors of epithelial origin usually appear as simple or complex cystic masses and account for the majority of ovarian neoplasms. The most frequent benign cystic ovarian tumors are represented by serous and mucinous cystadenomas. Serous cystadenoma typically appears as a unilocular or multilocular cystic mass with homoge-

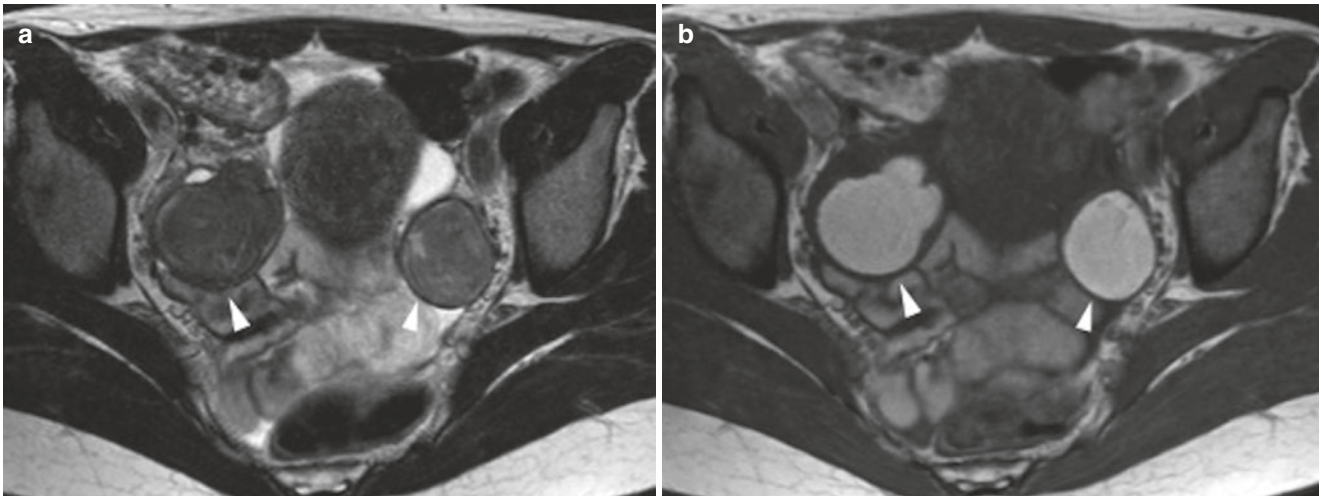


Fig. 15.22 Ovarian endometriomas. T2-weighted image (a) and fat-suppressed T1-weighted image (b) are shown. Bilateral ovarian cystic masses (white arrowheads) demonstrate hemorrhagic content with high

signal intensity on T1-weighted image and low signal intensity on T2-weighted images. These findings are typical of endometriotic cysts

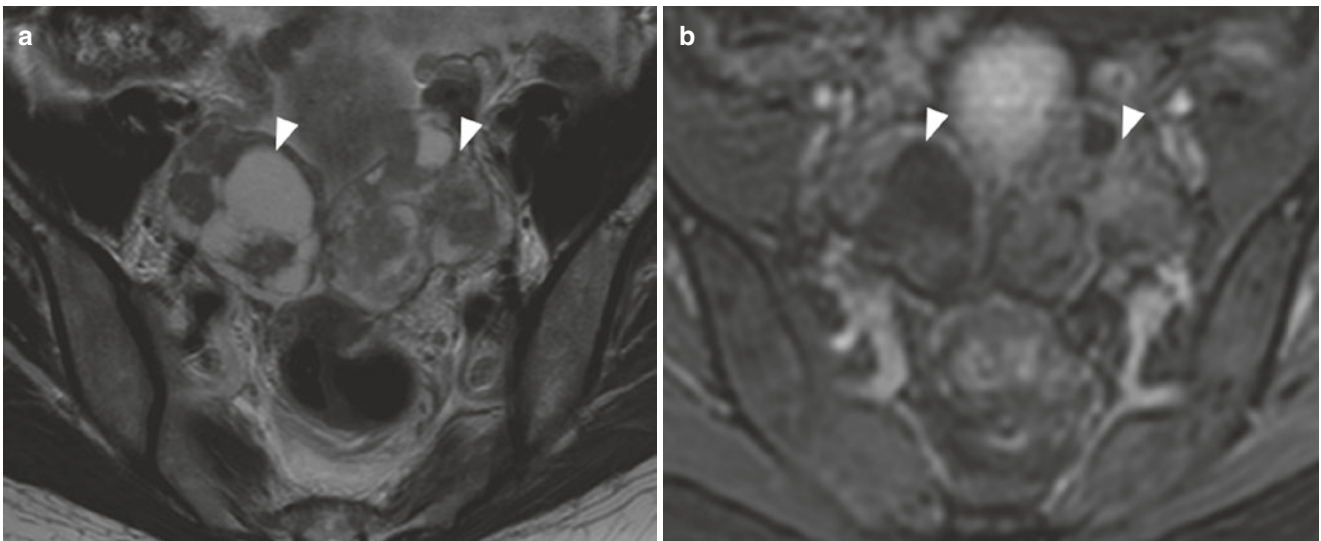


Fig. 15.23 Ovarian serous cystadenocarcinoma. T2-weighted image (a) and contrast-enhanced image (b) are shown. Bilateral adnexal complex masses with solid and cystic components (white arrowheads) are typical of malignant ovarian tumors

neous fluid content, thin walls, and fine internal septa. Mucinous cystadenoma usually presents as a multilocular cystic mass with heterogeneous appearance due to variable signal characteristics of the fluid loculations that frequently contain different amounts of proteinaceous or mucinous material. In the evaluation of ovarian cystic masses, the presence of thick enhancing walls and septations (more than 3 mm thick) and intracystic papillary projections should suggest a borderline or malignant tumor. A complex cystic mass with large solid components is highly suspicious for ovarian carcinoma (Fig. 15.23), especially if associated with intralesional necrotic changes or peritoneal effusion.

Solid Masses

Predominantly solid ovarian masses account for a small proportion of ovarian tumors. Fibrotic ovarian tumors of sex cord-stromal origin, constituted by the spectrum of related pathological entities of the fibroma-thecoma group, typically appear as masses with predominantly low signal intensity on T2-weighted images. These lesions may contain areas of high signal intensity on T2-weighted images attributable to stromal edema or cystic changes, more frequently found in tumors with prevalent thecoma features. Pure thecomas tend to appear as masses with a heterogeneous high signal on T2-weighted images and are often indistinguishable from malignant solid tumors. Brenner tumors are benign masses

of transitional cell origin that can show similar signal characteristics as fibromas when mainly solid or appearing as multilocular cystic masses with solid fibrous components. A useful distinguishing feature from other fibrous masses is the presence of calcification in the solid portions of the tumor, better recognizable by CT. Granulosa cell tumors are rare neoplasms of sex cord-stromal origin with indolent but potentially malignant behavior and variable imaging features. These tumors can appear as predominantly solid masses but also as multilocular cystic masses with minimal or no solid component that may be difficult to distinguish from more common ovarian epithelial tumors. A typical imaging finding in multilocular granulosa cell tumors is the presence of intracystic hemorrhage with high signal intensity areas on T1-weighted images and fluid-fluid levels.

Key Learning Points

- Endometriomas typically appear as hemorrhagic cysts with low signal intensity on T2-weighted images.
- Mature cystic teratomas typically appear as cystic fat-containing masses.
- Ovarian tumors of epithelial origin usually appear as simple or complex cystic masses. Serous cystadenomas often appear as unilocular simple cysts, whereas mucinous cystadenomas usually appear as multilocular cysts with fluid loculations having variable signal intensity. Malignant ovarian tumors typically contain papillary projections or solid components.
- Fibrotic ovarian neoplasms like fibroma-thecomomas and Brenner tumors typically show low signal intensity on T2-weighted images. Granulosa cell tumors may sometimes appear as multicystic masses with hemorrhage and fluid-fluid levels.

15.4.4.8 Evaluation of Bone and Soft Tissue Lesions

Bone Marrow Signal Alterations

Bone marrow is mainly composed of a mixture of hematopoietic tissue, more represented in red marrow, and adipose tissue that makes up the majority of yellow marrow. Yellow marrow has the same signal intensity of fat on T1-weighted, T2-weighted, and STIR images. Red marrow typically has a lower signal intensity than fat on T1-weighted images but higher than muscle tissue or intervertebral disks. On T2-weighted images, red marrow shows a lower signal than fat and a slightly higher signal compared to muscle, while on

STIR or fat-suppressed T2-weighted images, it exhibits intermediate signal intensity. The relative proportion of hematopoietically active red marrow is age-dependent, highest at birth, and gradually decreasing from childhood to adulthood. Physiological conversion of red marrow to yellow marrow starts from the limbs and progresses centrally until the adult pattern is reached. In adults red bone marrow is typically confined to axial skeleton, including the spine and the subchondral bone of the humeral and femoral proximal extremities. Reconversion of yellow to red marrow, a physiological reaction to a variety of stimuli, consists of the reappearance of red marrow in adult skeleton in places formerly occupied by yellow marrow. Reconversion tends to appear symmetrical, showing the typical characteristics of normal red marrow and need not to be confused with replacement of the bone marrow by pathological tissue. Patchy areas of normal red marrow in vertebral bodies may at times mimic a focal lesion. The occasional presence of a small adipose focus (so-called “bull’s eye” sign) inside red marrow areas may suggest the correct diagnosis.

Bone marrow edema is a very common but unspecific alteration that can be found in association with a wide variety of conditions including traumatic, inflammatory, vascular, degenerative, neoplastic, and metabolic. Edema shows high signal intensity on STIR and T2-weighted images and hypointensity on T1-weighted images, often appearing as hazy reticular signal alterations intermixed with normal bone marrow. In very mild cases, bone edema is detectable on STIR and fat-suppressed T2-weighted images with minimal signal alterations on T1-weighted images. Bone marrow edema associated with degenerative articular changes typically involves the subchondral bone. In degenerative disk disease, variable signal changes of vertebral bodies along the endplates are a common occurrence; they may be caused by reactive vascularized tissue fissuring the endplate and invading the adjacent vertebral body (low signal intensity on T1- and high signal intensity on T2-weighted and STIR images), prevalent fatty infiltration (high signal intensity in both T1-weighted and T2-weighted images with signal suppression on STIR), and subchondral bone sclerosis (low signal intensity in T1- and T2-weighted images).

A wide range of both benign and malignant diseases that affect the bone may appear as focal lesions (solitary or multiple), diffuse signal alterations, or aggressive bone destructive processes with extraosseous involvement. Hemangioma is a very common benign focal lesion often located in vertebral bodies that typically appear as a predominantly fat-containing mass, with signal comparable to that of adipose tissue. A minority of hemangiomas contain small amounts of fat and may be difficult to distinguish from malignant disease because of their unspecific signal intensity (low signal in T1-weighted and high signal in T2-weighted and STIR images). Enchondroma is another type of benign bone tumor

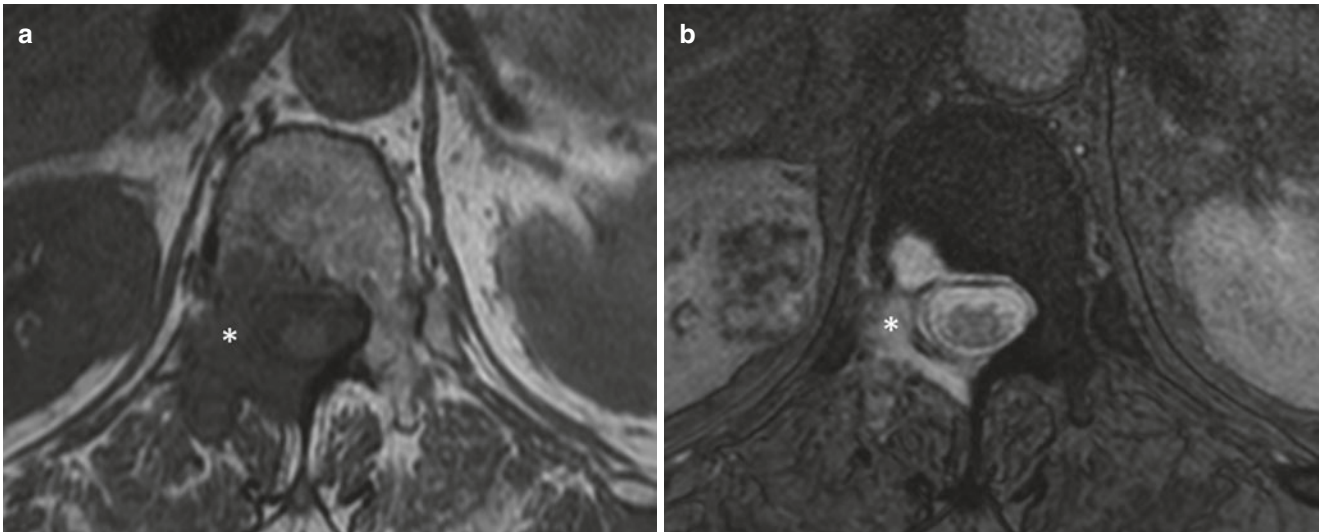


Fig. 15.24 Vertebral metastasis in patient with renal cell carcinoma. T1-weighted image (a) and gradient-echo T2*-weighted image (b) are shown. A destructive bone lesion is seen in the right vertebral pedicle

and lamina partially involving the posterior vertebral body (white asterisk) with extraosseous extension

often incidentally discovered in long bones. The typical imaging appearance of enchondroma is a lobulated intramedullary mass with low signal intensity on T1-weighted images and markedly high signal intensity on T2-weighted images that may contain foci of very low signal due to calcification. Bone cystic lesions often have similar characteristics as cysts found in other anatomical sites. Aneurysmal bone cyst is a lesion that may arise in bone as an isolated alteration or in association with other benign and malignant tumors and is characterized by multiple loculations containing fluid-fluid levels of variable signal intensity due to the presence of hemorrhage.

In aggressive bone diseases such as osteomyelitis and neoplasms, the normal bone marrow is replaced by pathological tissue that shows high signal intensity on T2-weighted and STIR images, lower signal intensity compared with bone edema on T1-weighted images and typically exhibits contrast enhancement. In infectious processes like osteomyelitis and spondylodiscitis, cortical bone destruction may be associated with the presence of fluid collections that can involve surrounding soft tissues. In malignant neoplasms arising primarily in the bones, the signal intensity of the tumor can be variable, reflecting different pathological features. Extraosseous involvement with local soft tissue invasion is a common occurrence in primary bone tumors but can also be seen in metastatic bone disease (Fig. 15.24). Metastases often appear as well-demarcated focal lesions with variable pattern of skeletal involvement and signal characteristics similar to other bone replacement processes. Less frequently osteoblastic metastases may demonstrate low signal intensity in all imaging sequences due to the prevalence of sclerotic bone over tumor tissue; in these cases they can be

undetectable on STIR images but are easily recognizable on T1-weighted images. Sometimes metastatic disease may appear as disseminated multinodular or diffuse bone marrow replacement that is better seen on T1-weighted sequences, especially in the spine where signal intensity of vertebral bodies and posterior elements may be lower than the signal intensity of normal intervertebral disks. The different patterns of metastatic bone involvement are nonspecific and can be found in other malignant infiltrative processes such as leukemia/lymphoma and multiple myeloma.

Soft Tissue Masses with Typical Imaging Features

Soft tissue masses are lesions originating from mesenchyme-derived connective tissues. A few common soft tissue masses present with some specific imaging features that are useful for their characterization. Lipoma is the most frequently encountered benign soft tissue lesion, typically appearing as a mass composed entirely of fat. A minority of lipomas may show thin internal septations that appear hypointense compared to fat or may contain non-adipose tissue components mostly represented by degenerative changes like fibrosis, liponecrosis, calcification, and myxoid degeneration. These complex-appearing lipomas may be difficult to distinguish from well-differentiated liposarcomas (Fig. 15.4). The presence of thick nodular septations or non-fatty solid areas should raise the suspicion of malignancy. Poorly differentiated liposarcomas often appear as completely solid lesions with minimal fat, at times detectable only on dual-phase chemical shift imaging, and have variable signal intensity reflecting pathological features (myxomatous variants typically show high signal intensity on T2-weighted images). Lipomas may

arise in superficial or deep compartments, the latter including mediastinal and retroperitoneal lipomatous tumors that carry a worse prognosis compared to superficial masses. Peripheral nerve sheath tumors are neurogenic masses mainly represented by schwannomas and neurofibromas, the main difference being their relationship with nerve fibers. These tumors share similar imaging findings and cannot be easily differentiated from each other based on imaging alone. Both lesions typically appear as elongated solid masses oriented parallel to the nerve with smooth contours, hyperintense on T2-weighted images and nearly isointense compared to muscle on T1-weighted images, often surrounded by a rim of normal fat tissue (so-called split fat sign). In imaging planes oriented perpendicular to the tumor long axis, an area of low signal intensity on T2-weighted images can sometimes be appreciated in the central portion (so-called target sign) attributable to collagenous fibrous tissue; this imaging appearance is more commonly seen in neurofibroma but is not a reliable distinguishing feature. It is not uncommon for peripheral nerve sheath tumors to show inhomogeneous signal on T2-weighted images with fluid-like intralesional components due to myxoid degeneration and cystic changes. These lesions may demonstrate variable degrees of contrast enhancement. Elastofibroma dorsi is a benign mass composed of fibroelastic tissue (nearly isointense to muscle on T1- and T2-weighted images) intermixed with linear fat components that give the classic striated appearance. Hemangiomas arising in soft tissues may have variable signal characteristics depending on pathological features. Most lesions are composed predominantly of dilated vessels with slow-flowing blood, showing high signal intensity on T2-weighted images and variable enhancement on post-contrast images. Internal foci of low T2 signal intensity may be generated by flow voids in areas of rapidly flowing blood or more typically by phleboliths. Hemangiomas may also contain fat, fibrous, or hemorrhagic components that have typical signal intensities. Gradient-echo T2*-weighted images are useful to detect the presence of hemosiderin within hemangiomas and to help characterize other soft tissue masses that contain large amounts of hemosiderin, such as giant cell tumors. Pure cystic lesions of soft tissues are readily recognized by their typical appearance and specific location: synovial cysts, ganglia, and clear fluid collections. Myxomatous tumors, both benign and malignant, may at times appear as cyst-like masses due to high signal intensity on T2-weighted images and hypointensity on T1-weighted images. The presence of contrast enhancement, often of low intensity, is useful to distinguish myxomatous lesions from cysts. Soft tissue sarcomas in most cases appear as inhomogeneous predominantly solid enhancing masses with unspecific signal intensity on T1- and T2-weighted images. Intralesional cystic, necrotic,

myxoid, and hemorrhagic changes can further complicate the imaging appearance. Synovial sarcoma is a relatively common malignant neoplasm often arising in soft tissues near large joints, more frequently around the knee. It may show typical although non-pathognomonic imaging findings: marked heterogeneous signal on T2-weighted images due to the admixture of necrotic and hemorrhagic areas (very high T2 signal intensity), solid enhancing tissue (intermediate T2 signal intensity), and fibrotic changes with calcifications (low T2 signal intensity) creating the so-called “triple sign”. In a minority of cases, synovial sarcoma shows a multiloculated appearance (so-called “bowl of grapes”) due to clustering of multiple cystic areas that contain fluid-fluid levels with variable signal intensities due to hemorrhage.

Key Learning Points

- Red marrow shows lower signal intensity compared to yellow fatty marrow.
- Bone marrow edema shows high signal intensity on fat-suppressed T2-weighted and STIR images.
- Benign bone lesions like cysts and enchondromas typically show very high signal intensity on T2-weighted images.
- Vertebral hemangiomas usually appear as macroscopic fat-containing masses.
- Aggressive bone diseases, like infectious processes and malignant primary and secondary neoplasms, usually show low signal intensity on T1-weighted images.
- Lipomas typically appear as masses composed entirely of macroscopic fat. Liposarcomas often appear as fat-containing lesions with thick nodular septations and solid non-fatty components.
- Schwannomas and neurofibromas usually appear as high signal intensity masses on T2-weighted images, sometimes with myxoid and cystic changes.
- Soft tissue hemangiomas typically appear markedly hyperintense on T2-weighted images. Signal voids from fast-flowing blood or phleboliths may be present.
- Cystic and myxomatous lesions show very high signal intensity on T2-weighted images and can be differentiated from each other on contrast-enhanced images.
- Soft tissue sarcomas show variable signal characteristics.
- Some tumors, such as synovial sarcomas, may sometimes show typical, although non-pathognomonic, imaging features.

Further Reading

- Ackman JB, Wu CC. MRI of the thymus. *AJR Am J Roentgenol.* 2011;197(1):W15–20.
- Albiin N. MRI of focal liver lesions. *Curr Med Imaging Rev.* 2012;8(2):107–16.
- Allen BC, Hosseinzadeh K, Qasem SA, et al. Practical approach to MRI of female pelvic masses. *AJR Am J Roentgenol.* 2014;202(6):1366–75.
- Baliyan V, Das CJ, Sharma R, et al. Diffusion weighted imaging: technique and applications. *World J Radiol.* 2016;8(9):785–98.
- Bangiyev L, Rossi Espagnet MC, Young R, et al. Adult brain tumor imaging: state of the art. *Semin Roentgenol.* 2014;49:39–52.
- Bitar R, Leung G, Perng R, et al. MR pulse sequences: what every radiologist wants to know but is afraid to ask. *Radiographics.* 2006;26(2):513–37.
- Blake MA, Cronin CG, Boland GW. Adrenal imaging. *AJR Am J Roentgenol.* 2010;194(6):1450–60.
- Chundru S, Kalb B, Arif-Tiwari H, et al. MRI of diffuse liver disease: characteristics of acute and chronic diseases. *Diagn Interv Radiol.* 2014;20(3):200–8.
- Del Grande F, Farahani SJ, Carrino JA, et al. Bone marrow lesions: a systematic diagnostic approach. *Indian J Radiol Imaging.* 2014;24(3):279–87.
- Elsayes KM, Mukundan G, Narra VR, et al. Adrenal masses: MR imaging features with pathologic correlation. *Radiographics.* 2004;24(Suppl 1):S73–86.
- Foti PV, Attinà G, Spadola S, et al. MR imaging of ovarian masses: classification and differential diagnosis. *Insights Imaging.* 2016;7(1):21–41.
- Freire M, Remer EM. Clinical and radiologic features of cystic renal masses. *AJR Am J Roentgenol.* 2009;192:1367–72.
- Ginat DT, Meyers SP. Intracranial lesions with high signal intensity on T1-weighted MR images: differential diagnosis. *Radiographics.* 2012;32:499–516.
- Hanrahan CJ, Shah LM. MRI of spinal bone marrow: part 2, T1-weighted imaging-based differential diagnosis. *AJR Am J Roentgenol.* 2011;197(6):1309–21.
- Hoang JK, Vanka J, Ludwig BJ, et al. Evaluation of cervical lymph nodes in head and neck cancer with CT and MRI: tips, traps, and a systematic approach. *AJR Am J Roentgenol.* 2013;200(1):W17–25.
- Inaoka T, Takahashi K, Mineta M, et al. Thymic hyperplasia and thymus gland tumors: differentiation with chemical shift MR imaging. *Radiology.* 2007;243(3):869–76.
- Juanpere S, Cañete N, Ortuño P, et al. A diagnostic approach to the mediastinal masses. *Insights Imaging.* 2013;4(1):29–52.
- Kakkar C, Shetty CM, Koteswara P, et al. Telltale signs of peripheral neurogenic tumors on magnetic resonance imaging. *Indian J Radiol Imaging.* 2015;25(4):453–8.
- Kalb B, Sarmiento JM, Kooby DA, et al. MR imaging of cystic lesions of the pancreas. *Radiographics.* 2009;29(6):1749–65.
- Khosa F, Khan AN, Eisenberg RL. Hypervascular liver lesions on MRI. *AJR Am J Roentgenol.* 2011;197(2):W204–20.
- Lee KY, Oh YW, Noh HJ, et al. Extraadrenal paragangliomas of the body: imaging features. *AJR Am J Roentgenol.* 2006;187(2):492–504.
- Matos AP, Velloni F, Ramalho M, et al. Focal liver lesions: practical magnetic resonance imaging approach. *World J Hepatol.* 2015;7(16):1987–2008.
- McInnis MC, Flores EJ, Shepard JA, Ackman JB. Pitfalls in the imaging and interpretation of benign thymic lesions: how thymic MRI can help. *AJR Am J Roentgenol.* 2016;206(1):W1–8.
- Miller FH, Rini NJ, Keppke AL. MRI of adenocarcinoma of the pancreas. *AJR Am J Roentgenol.* 2006;187(4):W365–74.
- Mittal MK, Malik A, Sureka B, et al. Cystic masses of neck: a pictorial review. *Indian J Radiol Imaging.* 2012;22(4):334–43.
- Nakazono T, White CS, Yamasaki F, et al. MRI findings of mediastinal neurogenic tumors. *AJR Am J Roentgenol.* 2011;197(4):W643–52.
- Nascimento D, Suchard G, Hatem M, et al. The role of magnetic resonance imaging in the evaluation of bone tumours and tumour-like lesions. *Insights Imaging.* 2014;5(4):419–40.
- Nikken JJ, Krestin GP. MRI of the kidney—state of the art. *Eur Radiol.* 2007;17(11):2780–93.
- Nouh MR, Eid AF. Magnetic resonance imaging of the spinal marrow: basic understanding of the normal marrow pattern and its variant. *World J Radiol.* 2015;7(12):448–58.
- Ödev K, Arıbaş BK, Nayman A, et al. Imaging of cystic and cyst-like lesions of the mediastinum with pathologic correlation. *J Clin Imaging Sci.* 2012;2:33.
- Palas J, Matos AP, Ramalho M. The spleen revisited: an overview on magnetic resonance imaging. *Radiol Res Pract.* 2013;2013:219297.
- Pedrosa I, Sun MR, Spencer M, et al. MR imaging of renal masses: correlation with findings at surgery and pathologic analysis. *Radiographics.* 2008;28(4):985–1003.
- Puderbach M, Hintze C, Ley S, et al. MR imaging of the chest: a practical approach at 1.5T. *Eur J Radiol.* 2007;64(3):345–55.
- Revelli M, Chiesa F, Del Prato A, et al. Role of respiratory-triggered diffusion-weighted MRI in the assessment of pleural disease. *Br J Radiol.* 2016:20160289.
- Sandrasegaran K, Lin C, Akisik FM, et al. State-of-the-art pancreatic MRI. *AJR Am J Roentgenol.* 2010;195:42–53.
- Schima W. MRI of the pancreas: tumours and tumour-simulating processes. *Cancer Imaging.* 2006;6(1):199–203.
- Shah LM, Hanrahan CJ. MRI of spinal bone marrow: part I, techniques and normal age-related appearances. *AJR Am J Roentgenol.* 2011;197(6):1298–308.
- Sharma V, Prabhaskar K, Noronha V, et al. A systematic approach to diagnosis of cystic brain lesions. *South Asian J Cancer.* 2013;2(2):98–101.
- Smirniotopoulos JG, Murphy FM, Rushing EJ, et al. Patterns of contrast enhancement in the brain and meninges. *Radiographics.* 2007;27(2):525–51.
- Stadnik TW, Demaerel P, Luybaert RR, et al. Imaging tutorial: differential diagnosis of bright lesions on diffusion-weighted MR images. *Radiographics.* 2003;23(1):e7.
- Takahashi K, Al-Janabi NJ. Computed tomography and magnetic resonance imaging of mediastinal tumors. *J Magn Reson Imaging.* 2010;32(6):1325–39.
- Tani I, Kurihara Y, Kawasuchi A, et al. MR imaging of diffuse liver disease. *AJR Am J Roentgenol.* 2000;174:965–71.
- Thoeny HC. Imaging of salivary gland tumours. *Cancer Imaging.* 2007;7(1):52–62.
- Vancouwenberghe T, Snoeckx A, Vanbeckevoort D, et al. Imaging of the spleen: what the clinician needs to know. *Singap Med J.* 2015;56(3):133–44.
- Zimny A, Neska-Matuszewska M, Bładowska J, et al. Intracranial lesions with low signal intensity on T2-weighted MR images – review of pathologies. *Pol J Radiol.* 2015;80:40–50.